

This article was downloaded by: [Diego Pol]

On: 05 March 2012, At: 07:36

Publisher: Taylor & Francis

Informa Ltd Registered in England and Wales Registered Number: 1072954 Registered office: Mortimer House, 37-41 Mortimer Street, London W1T 3JH, UK



Journal of Vertebrate Paleontology

Publication details, including instructions for authors and subscription information:

<http://www.tandfonline.com/loi/ujvp20>

Postcranial anatomy of *Sebecus icaeorhinus* (Crocodyliformes, Sebecidae) from the Eocene of Patagonia

Diego Pol^a, Juan M. Leardi^b, Agustina Lecuona^a & Marcelo Krause^a

^a CONICET, Museo Paleontológico Egidio Feruglio, Avenida Fontana 140, Trelew, 9100, Chubut, Argentina

^b CONICET, IDEAN, Departamento de Ciencias Geológicas, Facultad de Ciencias Exactas y Naturales, Universidad de Buenos Aires, Intendente Güiraldes 2160, Ciudad Universitaria, Buenos Aires, 1428, Argentina

Available online: 28 Feb 2012

To cite this article: Diego Pol, Juan M. Leardi, Agustina Lecuona & Marcelo Krause (2012): Postcranial anatomy of *Sebecus icaeorhinus* (Crocodyliformes, Sebecidae) from the Eocene of Patagonia, *Journal of Vertebrate Paleontology*, 32:2, 328-354

To link to this article: <http://dx.doi.org/10.1080/02724634.2012.646833>

PLEASE SCROLL DOWN FOR ARTICLE

Full terms and conditions of use: <http://www.tandfonline.com/page/terms-and-conditions>

This article may be used for research, teaching, and private study purposes. Any substantial or systematic reproduction, redistribution, reselling, loan, sub-licensing, systematic supply, or distribution in any form to anyone is expressly forbidden.

The publisher does not give any warranty express or implied or make any representation that the contents will be complete or accurate or up to date. The accuracy of any instructions, formulae, and drug doses should be independently verified with primary sources. The publisher shall not be liable for any loss, actions, claims, proceedings, demand, or costs or damages whatsoever or howsoever caused arising directly or indirectly in connection with or arising out of the use of this material.

POSTCRANIAL ANATOMY OF *SEBECUS ICAEORHINUS* (CROCODYLIFORMES, SEBECIDAE) FROM THE EOCENE OF PATAGONIA

DIEGO POL,^{*1} JUAN M. LEARDI,² AGUSTINA LECUONA,¹ and MARCELO KRAUSE¹

¹CONICET, Museo Paleontológico Egidio Feruglio, Avenida Fontana 140, Trelew 9100, Chubut, Argentina, dpol@mef.org.ar; alecuona@mef.org.ar; mkrause@mef.org.ar;

²CONICET, IDEAN, Departamento de Ciencias Geológicas, Facultad de Ciencias Exactas y Naturales, Universidad de Buenos Aires, Intendente Güiraldes 2160, Ciudad Universitaria, Buenos Aires 1428, Argentina, juanmartinleardi@gmail.com

ABSTRACT—We describe postcranial remains of new specimens referred to *Sebecus icaeorhinus* found in the lower section of the Sarmiento Formation at Cañadón Hondo (central Patagonia, Argentina), commonly regarded as part of the Casamayoran South American Land Mammal Age (middle Eocene). The new specimens include a partially articulated postcranium associated with teeth and fragmentary remains of the mandible that allows their identification as *S. icaeorhinus*. This taxon was almost exclusively known from skull remains from the same stratigraphic unit and was characterized by unique cranial features such as a long, high, and narrow rostrum bearing serrated teeth. The new material reveals numerous details on the postcranial anatomy of this crocodyliform, including the presence of proportionately long limbs and 10 autapomorphies in the vertebrae, forelimb, and pelvic girdle (some of which are interpreted as adaptations to terrestriality and an erect limb posture). These features depict a highly modified postcranial anatomy for *S. icaeorhinus* in comparison with that of neosuchian crocodyliforms, paralleling the uniqueness of its skull anatomy. The new information is also phylogenetically informative and incorporated into a cladistic analysis that corroborates not only the close affinities of Sebecidae with Baurusuchidae (sebecosuchian monophyly), but also the deeply nested position of this clade within Notosuchia. The incorporation of postcranial characters to the phylogenetic analysis also results in a novel arrangement of the basal mesoeucrocodylians recorded in the Cretaceous–Cenozoic of Gondwana, clustering all of these species into a large monophyletic clade.

INTRODUCTION

Sebecus icaeorhinus was originally named by Simpson (1937) in a brief paper following the discovery of an almost complete, but disarticulated, skull from the middle Eocene beds of the Sarmiento Formation, during the Scarritt Expeditions to Patagonia organized by the American Museum of Natural History. The type specimen of *S. icaeorhinus* (AMNH 3160) was found in the famous “Bird Clay” locality of Cañadón Hondo in Chubut Province (central Patagonia, Argentina). Later, Colbert (1946) described this specimen in detail and referred to *S. icaeorhinus* another specimen (AMNH 3159) consisting of fragmentary cranial and postcranial remains found in the Eocene beds of Cañadón Vaca. A third specimen referred to *S. icaeorhinus* (MMP 235) was subsequently found in Cañadón Vaca and described by Gasparini (1972), consisting of a fragmentary skull that added new information on the choanal morphology of this taxon (see also Molnar, 2010).

Since its original description, *Sebecus icaeorhinus* has drawn the attention of numerous authors because of its theropod-like teeth and unusual skull morphology (e.g., extremely narrow and high rostrum, wide choanal opening), leading to the recognition of this taxon and its allies (i.e., Sebecidae) as a distinctive group within Crocodyliformes (Simpson 1937; Colbert, 1946; Gasparini, 1972, 1984; Molnar, 2010). These autapomorphic characters were found in association with plesiomorphic characters (e.g., mesosuchian-type secondary palate), which suggested that *Sebecus* was more closely related to Cretaceous ‘mesosuchians’ (i.e., non-eusuchian mesoeucrocodylians) than to eusuchians (the

other group of crocodyliforms known from the Cenozoic of Patagonia).

During the last 25 years, several crocodyliform taxa from the Paleogene and early Neogene of South America have been described and referred to Sebecidae, comprising seven formally described taxa: *Sebecus icaeorhinus*, *Sebecus huilensis*, *Sebecus querejazus*, *Bretesuchus bonapartei*, *Barinasuchus arveloi*, *Ayllusuchus fernandezi*, and *Ilchuania parca* (Gasparini, 1984, 1996; Busbey, 1986; Buffetaut and Marshall, 1991; Gasparini et al., 1993; Langston and Gasparini, 1997; Paolillo and Linares, 2007; Molnar, 2010). The taxonomic diversity of Sebecidae may be even higher, however, because there are several forms yet to be described (Langston, 1965; Paula Couto, 1970; Gasparini, 1984). Sebecids were diverse and broadly distributed in South America and have been considered one of the major groups of carnivorous vertebrates during the Early Cenozoic of South America. Despite increased knowledge of sebecid diversity during the last several decades, the phylogenetic affinities of this group are still unresolved, with no current consensus on its evolutionary origins. Traditional hypotheses suggested affinities with two different groups of crocodyliforms from the Cretaceous of Gondwana: Baurusuchidae (forming the group Sebecosuchia; Colbert, 1946; Gasparini, 1972, 1984; Buffetaut, 1980) and Peirosauridae or ‘trematochampsids’ (Buffetaut, 1991; conforming to the monophyletic Sebecia sensu Larsson and Sues, 2007). Recent cladistic analyses have mirrored these ideas, alternatively retrieving Sebecidae as the sister group of Baurusuchidae (Ortega et al., 1996, 2000; Sereno et al., 2001, 2003; Pol et al., 2004, 2009; Pol and Apesteguía, 2005; Turner and Calvo, 2005; Gasparini et al., 2006) or Peirosauridae (Larsson and Sues, 2007; Sereno and Larsson, 2009).

Here, we report and describe new specimens found in Cañadón Hondo that include fragmentary mandibular remains and teeth,

*Corresponding author.

but remarkably complete and well-preserved postcranial material. These specimens are highly relevant because most of our current knowledge of *S. icaeorhinus* is based on its unusual craniomandibular morphology, whereas its postcranial anatomy is almost completely unknown and restricted to fragmentary remains. The lack of knowledge on the postcranial anatomy in *S. icaeorhinus* is paralleled in other taxa referred to Sebecidae, which are also almost exclusively known from craniomandibular remains. Therefore, the specimens described here, and the new anatomical information on *S. icaeorhinus*, are also relevant for understanding the poorly known postcranial anatomy of Sebecidae and evaluating the phylogenetic affinities of this enigmatic group of Cenozoic South American crocodyliforms.

Institutional Abbreviations—AMNH, American Museum of Natural History, New York, U.S.A.; GPIT, Institut und Museum für Geologie und Paläontologie, Universität Tübingen, Tübingen, Germany; IVPP, Institute of Vertebrate Paleontology and Paleoanthropology, Beijing, China; MACN, Museo Argentino de Ciencias Naturales, Buenos Aires, Argentina; MCF, Museo Carmen Funes, Plaza Huincul, Argentina; MMP, Museo de Historia Natural “Galileo Scaglia,” Mar del Plata, Argentina; MPEF, Museo Paleontológico Egidio Feruglio, Trelew, Argentina; MZSP, Museo Zoologia, Universidade de São Paulo, São Paulo, Brazil; SAM, Iziko-South African Museum, Cape Town, South Africa; UA, University of Antananarivo, Antananarivo, Madagascar; UAM, Universidad Autónoma de Madrid, Madrid, Spain; ZPAL, Instytut Paleobiologii PAN, Warsaw, Poland.

Anatomical Abbreviations—1sv, first sacral vertebra; aail, acetabular antitrochanter on ilium; aais, acetabular antitrochanter on ischium; ab, anterior bulge; ac, acetabulum; acr, anterior crest of the radiale; ah, anterior astragalar hollow; alpu, anterolateral process of the proximal end of the ulna; ampu, anteromedial process of the proximal end of the ulna; aop, anterior oblique process of the distal ulna; ap, anteroventral process of neural arch; asp, astagalar peg; as il, anterior articular surface for ilium; as is, anterior articular surface for ischium; as, astagalar articular surface; asu, articular surface for the radius; asul, articular surface for the ulna; atl, astragalar-tarsale ligament pit; cbd, insertion site of *M. coracobrachialis brevis dorsalis*; cbv, insertion site of *M. coracobrachialis brevis ventralis*; cc, calcaneal condyle; clt, crest of lateral tubercle; cs, calcaneal socket; di, diapophysis; dpc, deltopectoral crest; fc, fibula condyle; fcor, coracoid foramen; ffx, fossa flexoria; fs, fibular articular surface; ft, fourth trochanter; gl, glenoid; gt, greater trochanter; hy, hypapophysis; icg, intercondylar groove; ipd, infrapostzygapophyseal depression; ivc, incisura vertebralis cranialis; lhds, lateral margin of humeral distal shelf; lic, linea intermuscularis caudalis; lpra, lateral process of the proximal radius; lsc, lateral supracondylar ridge; lt, lateral tubercle; mhds, medial margin of humeral distal shelf; mi, depression for insertion of *M. caudifemoralis longus* and part of *M. puboischiofemoralis internus* 1; ml, medial lamina; mpc, medial proximal crest; mpra, medial process of the proximal radius; msc, medial supracondylar crest; n, notch separating the anterior edge of the tibial surface; ncs, neurocentral suture; ns, neural spine; oca, oblique crest of the articular surface for the scapula; ol, olecranon; pa, parapophysis; pbu, prezygapophyseal bulge; pef, prespinal fossa; pf, popliteal fossa; pg, posterior vertical groove on calcaneal tuber; pis dt3, proximally inset articular surface for distal tarsal 3; plas, planar astragalar surface; plcs, planar calcaneal surface; pmr, proximomedial process of the radiale; poas, posterior astragalar surface; pocs, posterior calcaneal surface; pod, posterior depression; pof, postspinal fossa; pog, postzygapophyseal groove; pop, posterior oblique process of the distal ulna; posp, postacetabular process; ppdl, parapodiapophyseal lamina; pr, parapophyseal ridge; prep, preacetabular process; prz, prezygapophysis; ps, pubic articular surface; ps il, posterior articular surface for ischium; pva, posteroventral projection of the proximal articular surface; pxas, proximal astragalar surface; pxcs, proximal calcaneal surface; pxd, proximal depression on astragalus; s 1r, articular surface for first sacral rib; s 2r, articular surface for second sacral rib; s cc, articular surface for the calcaneal condyle; s dt3, articular surface for distal tarsal 3; s dt4, articular surface for distal tarsal 4; s fc, articular surface for fibular condyle of femur; s fi?, articular surface for fibula?; s I, II, articular surface for metatarsals I and II; s mttV, articular surface for metatarsal V; s tc, articular surface for tibial condyle of femur; sac, supraacetabular crest; sg, shallow groove of the proximal ulna; shc, insertion site of the scapulohumeralis caudalis; sld, shallow lateral depression; ss, insertion site of the subscapularis; tbc, origin of the triceps brevis caudalis; tc, tibial condyle; ts, tibial articular surface; vf, vascular foramen; vfc, ventral fossa on calcaneum.

GEOLOGICAL SETTING

Cañadón Hondo is an erosional depression located 65 km to the north-northwest of Comodoro Rivadavia, Chubut, Argentina (Piatnitzky, 1931; Simpson, 1935; Andreis, 1977) (Fig. 1A). The sedimentary sequences that crop out in this area include, from base to top, the Salamanca Formation, the Río Chico Group and the Sarmiento and Chenque formations, all of them covered by the “Rodados Tehuelches” (Piatnitzky, 1931; Simpson, 1935; Feruglio, 1949; Andreis, 1977; Raigemborn et al., 2010) (Fig. 1B). The fossiliferous levels are located at the “Cerro Verde” locality on the western side of Cañadón Hondo (Schaeffer, 1947;

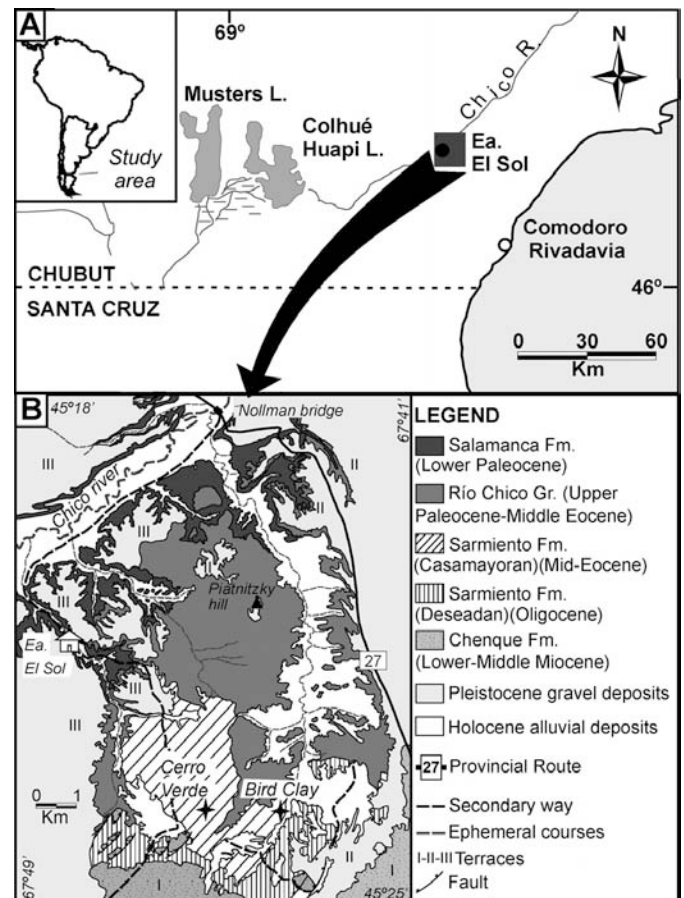


FIGURE 1. A, geographic location of the studied locality; B, simplified geologic map of the Cañadón Hondo area (modified from Andreis, 1977).

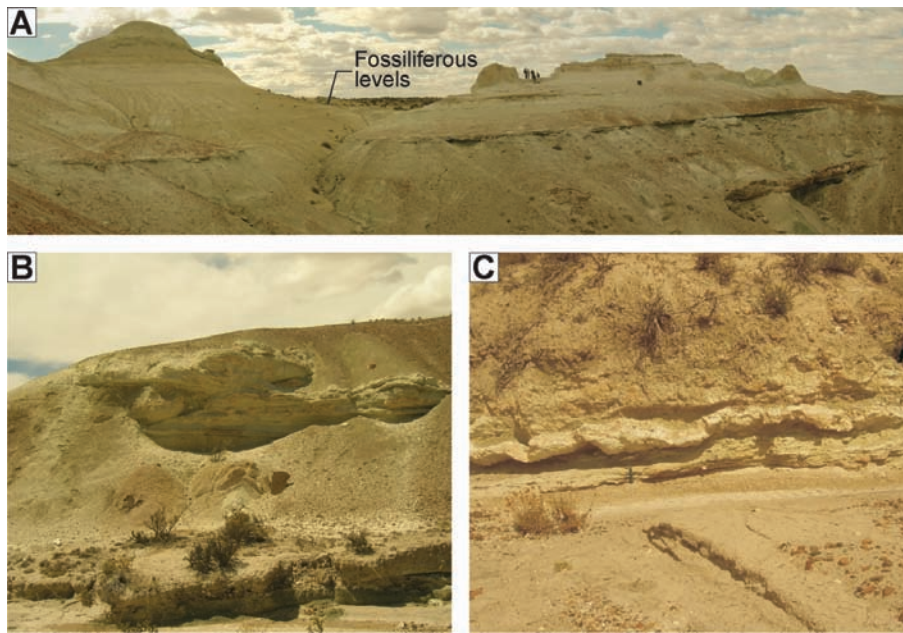


FIGURE 2. **A**, general view of the outcrops of the Sarmiento Formation in the middle-upper section at Cerro Verde; **B**, general view of the sequence of the Sarmiento Formation at the “Bird Clay” area, showing reverse faulting (the throw is approximately 70 cm); **C**, “Bird Clay” locality showing small-scale compactional folding on tuffs between near horizontal clayey levels (hammer for scale is 33 cm long). (Color figure available online.)

Andreis, 1977), where mudstones, sandstones, and tuffs of the Las Flores and Sarmiento formations crop out. The general geometry of the strata in this locality is characterized by tabular and slightly lenticular shapes, showing a general inclination of approximately 12° to the south-southwest. Two distinct fossiliferous levels were identified containing skeletal remains of sebecid crocodyliforms and turtles. The lowest level corresponds to a greenish tabular tuff, whereas the upper level is formed from a fine tuff with parallel lamination. These levels overlie a succession of massive and very fine tuffs, intercalated with indurated cornices showing trough-cross bedding. Immediately above the upper fossiliferous level there is a lenticular, massive sandstone bearing relative large (>1 cm) skeletal remains of mammals, referred by previous authors to the Casamayoran South American Land Mammal Age (SALMA: Simpson, 1935; Schaeffer, 1947; Andreis, 1977). Upward the section of the “Cerro Verde” culminates with 10–11 m of horizontally stratified, fine tuffs bearing small (<2 cm) skeletal remains, root traces, and massive and meniscate burrows. The holotype of *S. icaeorhinus* was found at the “Bird Clay” locality (Simpson, 1937; Schaeffer, 1947), located at the eastern flank of Cañadón Hondo. The fossiliferous levels at both localities (“Cerro Verde” and “Bird Clay”) are interpreted as equivalent in age, representing the lower levels of the Sarmiento Formation (Casamayoran SALMA, middle Eocene). The correlation between the rocks of the two localities is based on the consistency of the sedimentary features present, such as lithology, color, geometry, and the internal structures of the strata. The sequence exposed at and near the “Bird Clay” is also characterized by tabular and massive beds of greenish tuffs, clayey tuffs, and clay. In particular, the “Bird Clay” locality contains greenish, massive, clay-rich levels with intercalated white, usually deformed, tuffs, bearing avian, turtle, and crocodyliform remains (Simpson, 1937). We have recently relocated these exposures based on features discussed in Simpson’s field notes that were clearly recognized in outcrop (Fig. 2), although no further fossils were found at the “Bird Clay” locality. In addition to these observations, a geological map based on aerial photographs (Andreis, 1977) also indicates both localities have an equivalent stratigraphic position, the lowest section of the Sarmiento Formation (Fig. 1B).

SYSTEMATIC PALEONTOLOGY

CROCODYLOMORPHA Walker, 1970

CROCODYLIFORMES Hay, 1930 (sensu Clark, 1986)

SEBECOSUCHIA Simpson, 1937

SEBECIDAE Simpson, 1937

SEBECUS ICAEORHINUS Simpson, 1937
(Figs. 3–22)

Holotype—AMNH 3160, disarticulated skull and mandible.

Referred Specimens—AMNH 3159, fragmentary cranial remains associated with vertebral centrum and fragmentary femur and fibula; MMP 235, fragmentary skull; MPEF-PV 1776, partially articulated specimen including anterior region of the dentary and most of the postcranial skeleton; MPEF-PV 3970, cervical 3; MPEF-PV 3971, cervical 8; MPEF-PV 3972, proximal coracoid, distal humerus, proximal femur, astragali, and calcaneum belonging to at least two different individuals.

Locality and Horizon—AMNH 3160 was found in the “Bird Clay” locality of Cañadón Hondo. AMNH 3159 and MMP 235 were found in Cañadón Vaca. The specimens described here were found in the “Cerro Verde” locality, on the western margin of Cañadón Hondo. MPEF-PV 1776 was found in the upper level and MPEF-PV 3970–3972 were found in the lowermost fossiliferous levels of this locality (see Geological Settings). All the Cañadón Hondo specimens are regarded as coming from the lower levels of the Sarmiento Formation (see Geological Setting, above).

Emended Diagnosis—Mesoeucrocodylian crocodyliform diagnosed by the following unique combination of characters: rostrum mediolaterally compressed and dorsoventrally deep; choanal opening subcircular in shape and remarkably large, bounded by palatines anteriorly and pterygoids posteriorly; quadratojugal-surangular forming accessory craniomandibular articulation; distal body of quadrate bearing sharp ridge on posterior surface; four premaxillary, nine maxillary, and 13 dentary teeth; posterior teeth ziphodont and highly compressed mediolaterally; shallow notch at premaxillary-maxillary contact for reception of enlarged fourth dentary tooth. The postcranial remains bear diagnostic characters that are so far unique for *S. icaeorhinus*, although these could be diagnostic of a larger group

of sebecids given the lack of postcranial information for the group: markedly deep prespinal fossa in mid- to posterior cervical vertebrae, facing dorsally and well separated from anterior margin of neural arch; hypapophysis present in all cervicals and extending posteriorly to dorsal 6; coracoid shaft subcylindrical in cross-section; low deltopectoral crest that deflects medially along distal half; horizontal shelf above humeral condyles on anterior surface of humerus; articular surface for ulna on radiale mediolaterally narrow and dorsoventrally long; postacetabular process of ilium elongated, horizontal, and tapering posteriorly; posterior half of postacetabular process of ilium free of sacral rib attachment; iliac antitrochanter higher than anteroposteriorly long; shallow and smooth insertion area for *M. puboischiofemoralis internus* 1 (PIFI1) and *M. caudifemoralis longus* (CFL) anterior to fourth trochanter; absence of anterior ridge limiting calcaneal socket; absence of dorsolateral ridge on calcaneal tuber.

DESCRIPTION

The following description focuses primarily on the postcranial remains recovered at Cañadón Hondo housed in the MPEF collections, but associated mandibular remains and teeth are also described because these form the basis for referring these specimens to *S. icaeorhinus* (see below). Comparisons are made with other crocodyliforms for which the postcranium is known, with emphasis on basal mesoeucrocodylians. Sources of information on other taxa are detailed in Table 1. Unless otherwise noted, references to these taxa in the text are based on the literature or specimens listed in this table.

Mandible and Teeth

One of the new specimens (MPEF-PV 1776) preserves an anterior fragment of the dentary bearing two teeth. The external lateral surface of the dentary is flat, tall, and vertically oriented (Fig. 3), as in the holotype of *S. icaeorhinus* (Colbert, 1946; Molnar, 2010). The preserved anterior region of the dentary is strongly compressed mediolaterally as in *Sebecus*, but differing from the mediolaterally broad dentary of other sebecids (e.g., *Bretesuchus*). This fragment includes a dorsal projection of the alveolar margin that is slightly bulged laterally, as in the caniniform bearing region of the dentary of the holotype of *S. icaeorhinus* (AMNH 3160). The teeth are strongly compressed

TABLE 1. List of taxa used for comparisons in the text.

Taxon	Source
<i>Araripesuchus gomesii</i>	AMNH 24450
<i>Araripesuchus tsangatsangana</i>	Turner (2006)
<i>Baurusuchus albertoi</i>	Nascimento and Zaher (2010)
<i>Caiman latirostris</i>	MPEF-AC 205
<i>Chimaerasuchus paradoxu</i>	IVPP V 8274
<i>Edentosuchus tienshanensis</i>	IVPP V 3236
<i>Gobiosuchus kielanae</i>	ZPAL MgR-II/67
<i>Iberosuchus macrodon</i>	Ortega (2004)
<i>Lomasuchus palpebrosus</i>	MCF-PVPH 160
<i>Mahajangasuchus insignis</i>	UA 8654
<i>Malawisuchus mwakayasyunguti</i>	Gomani (1997)
<i>Mariliasuchus amarali</i>	MZSP-PV 50
<i>Notosuchus terrestris</i>	Pol (2005)
<i>Orthosuchus stormbergi</i>	SAM K 409
<i>Protosuchus richardsoni</i>	AMNH 3024
<i>Simosuchus clarki</i>	Georgi and Krause (2010), Sertich and Groenke (2010)
<i>Steneosaurus bollensis</i>	GPIT 1909 s.264
<i>Stratiosuchus maxhechti</i>	Riff (2007), Riff and Kellner (2011)
<i>Uruguaysuchus aznarezi</i>	Soto et al. (2011)

mediolaterally and are symmetrical along the labiolingual and mesiodistal planes, as in *Sebecus*, but contrasting with those of other ziphodont crocodyliforms (e.g., *Bretesuchus*, *Iberosuchus*, *Baurusuchus*; Riff and Kellner, 2001; Legasa et al., 1993). The mesial and distal margins of the teeth bear serrations that involve both the enamel and the dentine (i.e., ziphodont condition sensu Prasad and de Broin, 2002). The well-preserved distal margin bears 6–9 denticles per millimeter depending on the position along the margin (Fig. 3C). The depressions between denticles are broad, ‘U’-shaped, and lack the constriction towards the cutting edge of the crown present in other ziphodont taxa (see Legasa et al., 1993; Prasad and de Broin, 2002). These characters of the denticles distinguish the teeth of *Sebecus* from those of other ziphodont taxa. Given these similarities, the presence of *S. icaeorhinus* in equivalent levels of the Sarmiento Formation at the opposite margin of Cañadón Hondo, and the absence of other sebecid taxa from this unit, we refer MPEF-PV 1776 and the other material to *S. icaeorhinus*. Further discoveries of articulated cranial and postcranial remains at Cañadón Hondo will allow additional testing of this identification.

Axial Skeleton

Specimen MPEF-PV 1776 preserves 16 presacral vertebrae and the first sacral vertebra. The presacral vertebrae include the axis, five postaxial cervicals, and 10 dorsals. Two additional isolated vertebrae have also been recovered from the “Cerro Verde” area, identical in morphology but larger in size than those of MPEF-PV 1176. All vertebral centra are amphicoelous and anteroposteriorly longer than high or wide (see Supplementary Data; available online at www.tandfonline.com/UJVP), with the ventral surface of the centra moderately constricted at their midpoint.

Cervical Vertebrae—The preserved cervical vertebrae of MPEF-PV 1776 represent an almost complete cervical (C) series, missing only one element in addition to the atlas. Given the gradual change in the position of the parapophyses and diapophyses, the cervical remains of MPEF-PV 1776 are interpreted to represent a continuous series, from the axis to C7. Two isolated cervical centra also recovered from this locality are interpreted as C3 (MPEF-PV 3970) and C8 (MPEF-PV 3971) based on the position of the parapophysis and diapophysis.

The axis is represented by the intercentrum and the base of the neural arch only. The pedicles of the neural arch are approximately as long as the centrum but their anterior margins project

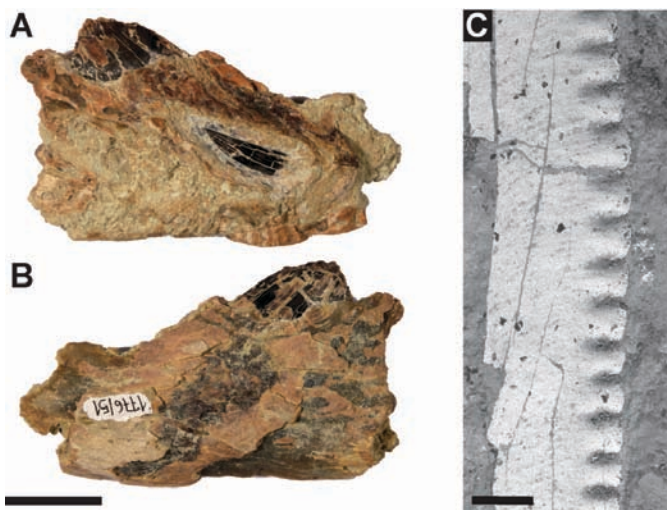


FIGURE 3. Mandibular remains of *S. icaeorhinus* (MPEF-PV 1776). **A**, right dentary in medial view showing replacement tooth; **B**, right dentary in lateral view; **C**, SEM image of distal margin of replacement tooth. Scale bars equal 1 cm (**A**, **B**), and 250 μ m (**C**). (Color figure available online.)

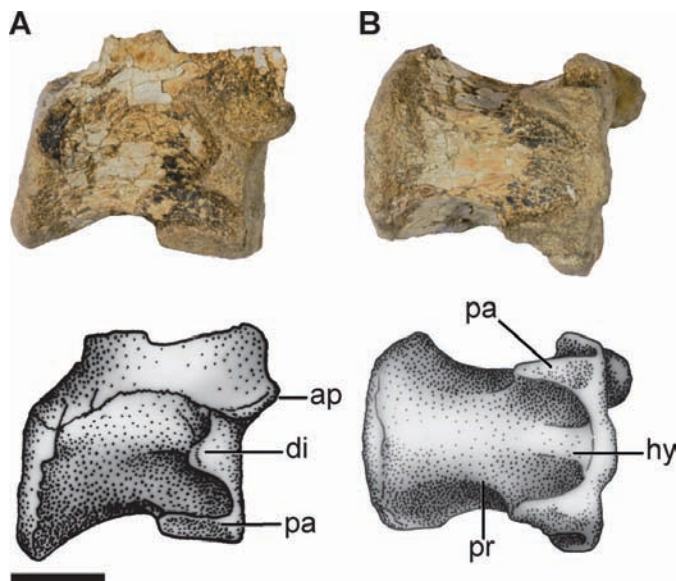


FIGURE 4. Axis of *S. icaeorhinus* (MPEF-PV 1776), in **A**, right lateral view; and **B**, ventral view. Scale bar equals 1 cm. (Color figure available online.)

farther anteriorly than the cranial margin of the centrum, likely contacting the dorsal surface of the unpreserved odontoid process (Fig. 4). Ventral to this point the anterodorsal corner of the axial centrum bears a flat and bifaceted articular surface. This

facet probably contacted the posterodorsal end of the odontoid process, and the two distinct articular facets suggest that it formed part of the diapophysis for the first cervical vertebra. This articular surface is subrectangular and dorsoventrally higher than anteroposteriorly long (Fig. 4). The parapophyses are located at the anterodorsal corner of the centrum and are dorsoventrally low and anteroposteriorly long. A short longitudinal ridge extends posteriorly from the caudal margin of the parapophysis along the lateral surface of the centrum (Fig. 4). This ridge defines the limit between the ventral and lateral surfaces of the axial centrum and disappears at the anteroposterior midpoint of the axis. Dorsal to the parapophyseal ridge, the excavated lateral surface of the centrum bears three small vascular foramina. The ventral surface of the centrum is mediolaterally constricted at its midpoint and flat, except for the hypapophysis on its anterior region (Fig. 4). The full ventral projection of the hypapophysis cannot be determined because its surface has been damaged by erosion. The anterior articular surface is flat and has a rugose surface denoting the attachment area for the odontoid process. The posterior articular surface is concave and is dorsoventrally taller than the anterior surface (see Supplementary Data).

C3 preserves only the centrum and the base of the neural arch. This element is dorsoventrally taller and anteroposteriorly longer than the axis (see Supplementary Data) and the neurocentral suture is still visible (Fig. 5). The posterior margin of the neural arch is markedly concave such that the posterior edge of the lateral wall of the neural canal is located more anteriorly than the posterior end of the centrum. The dorsal half of the diapophysis is located on the neural arch and its ventral half on the centrum (Fig. 5). It is centered on the anterior half of the vertebra, contrasting with the anteriorly placed diapophyses of other basal mesoeucrocodylians (e.g., *Simosuchus*). The diapophysis projects

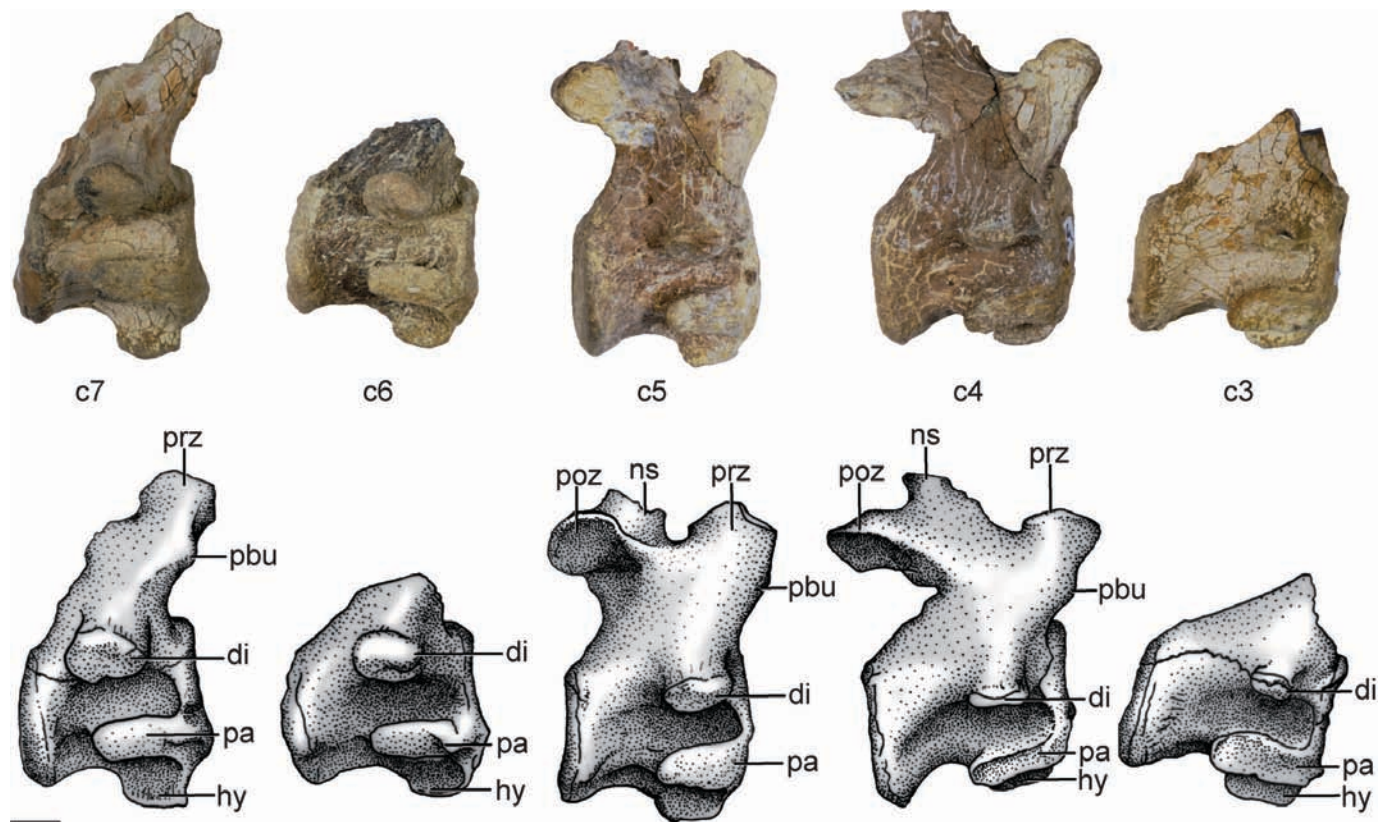


FIGURE 5. Cervical vertebrae 3–7 of *S. icaeorhinus* (MPEF-PV 1776) in right lateral view. C3 is on the right. Scale bar equals 1 cm. (Color figure available online.)

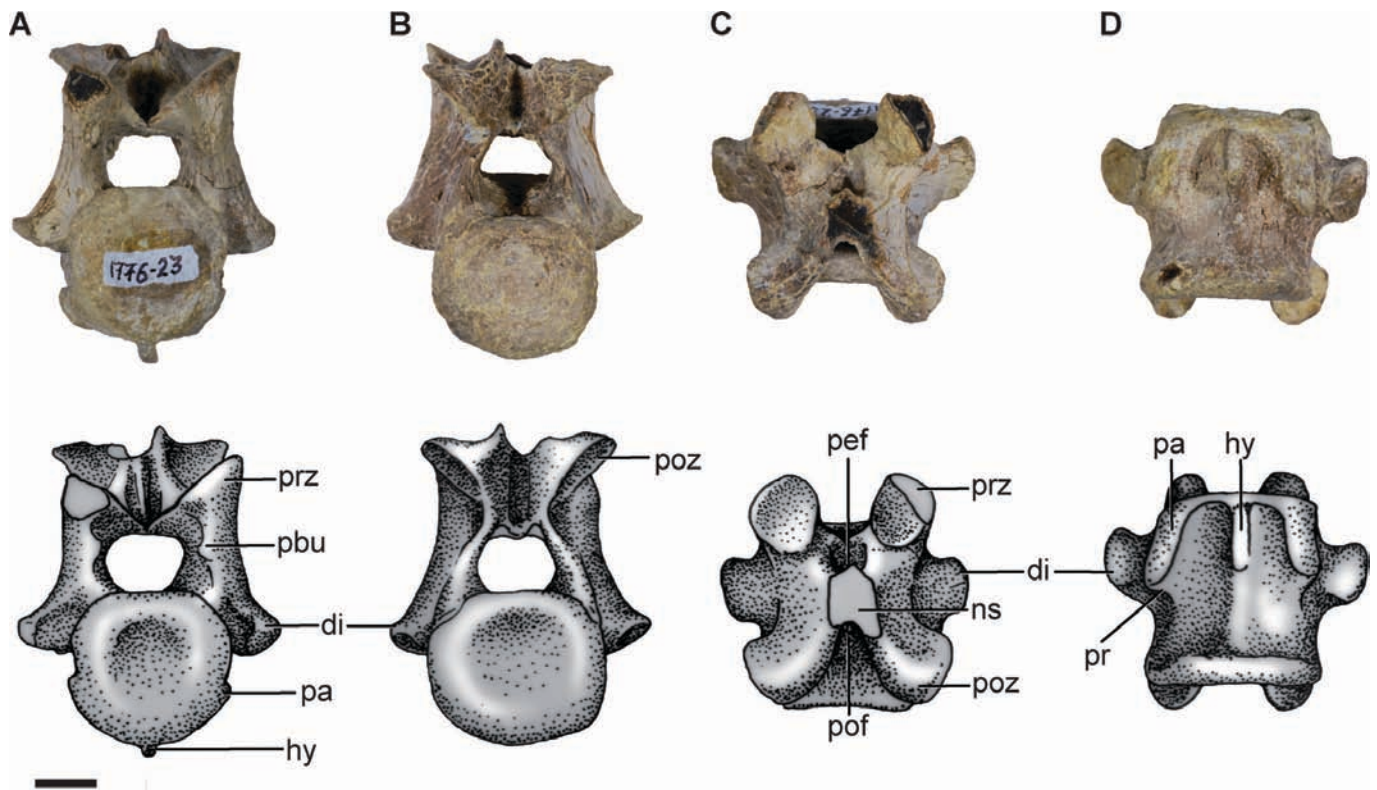


FIGURE 6. Cervical vertebra 5 of *S. icaeorhinus* (MPEF-PV 1776) in **A**, anterior view; **B**, posterior view; **C**, dorsal view; and **D**, ventral view. Scale bar equals 1 cm. (Color figure available online.)

ventrolaterally, bearing a rounded articular surface that is much smaller than in more posterior vertebrae. The parapophysis is ovoid in outline, with its major axis oriented longitudinally. Overall, the parapophysis is approximately three times larger than the diapophysis, extending along the anterior half of the vertebral centrum (Fig. 5). A reduced post-parapophyseal ridge is directed posteromedially from the posterior margin of the articular surface. The hypapophysis extends along the anterior one-third of the centrum, as a sagittally oriented lamina, subrectangular in lateral outline, and with its ventral-most region slightly expanded mediolaterally. The ventral surface of the centrum is flat posterior to the hypapophysis. The centrum is mediolaterally constricted at its midpoint with concave and subcircular articular surfaces. The posterior articular surface is mediolaterally broader than the anterior articular surface, a feature common to all of the other cervical vertebrae (Fig. 6).

C4 of MPEF-PV 1776 is almost completely preserved, lacking only the left postzygapophysis and the dorsal extent of the neural spine (Fig. 5). The neurocentral suture is closed, in contrast to the preceding vertebrae. As in C3, the neural arch is anterodorsally slanted. The neural spine is incomplete but its preserved base is anteroposteriorly short, as in *Notosuchus*, *Baurusuchus*, and *Simosuchus*. The spine is located over the posterior half of the neural arch (Fig. 5), contrasting with the anteroposteriorly centered neural spines of *Notosuchus*. The posterior edge of the neural spine projects between the bases of the postzygapophyses, suggesting the presence of an incipiently developed medial lamina. The anterior half of the dorsal surface of the neural arch is occupied by a prespinal fossa, a feature present in all preserved cervical neural arches (Fig. 6). This depression is a well-delimited deep fossa and is located at the midpoint between the neural spine and the prezygapophyses. A similar depression is also

present in other basal mesoeucrocodylians (e.g., *Iberosuchus*, *Mahajangasuchus*), although these are not as deep and well defined.

The prezygapophysis of C4 is dorsally directed, as in most basal mesoeucrocodylians (baurusuchids, *Notosuchus*, *Araripesuchus*, *Mahajangasuchus*). The anterior margin of the prezygapophyseal process is formed by a sharp ridge, as in *Notosuchus* but contrasting with the anteriorly convex process of crocodylians. This margin bears an anteriorly directed bulge that is present in all cervical vertebrae that preserve this region (Figs. 5, 6), which is also present in other basal mesoeucrocodylians (e.g., *B. albertoi*, *Mahajangasuchus*, *A. tsangatsangana*, *Iberosuchus*) but not in *Notosuchus*, *Uruguaysuchus*, *Simosuchus*, or *A. gomesii*. The medial surface of the prezygapophyseal process bears a shallow triangular depression between the bulge and the medial rim of the prezygapophyseal articular facet, as in several other basal mesoeucrocodylians (*B. albertoi*, *A. gomesii*, *A. tsangatsangana*, *Mahajangasuchus*). The articular facets of the prezygapophyses are subcircular, flat, and are oriented at approximately 45 degrees. The postzygapophysis is well separated from the neural spine, lacking the suprapostzygapophyseal lamina present in the cervicals of some notosuchids (Pol, 2005; Georgi and Krause, 2010).

The diapophysis of C4 is centered on the anterior half of the vertebra and projects lateroventrally, overhanging the centrum (Fig. 5). The articular facets of the diapophysis and parapophysis are similar to those of C3 (Fig. 5). The hypapophysis consists of a well-developed lamina, occupying the anterior one-third of the centrum, with a convex anterior margin and a concave posterior margin producing a slight posteroventral orientation. This contrasts with the anteroventrally projected hypapophysis of the middle-to-posterior cervicals of extant crocodylians. The lateral surfaces of the centrum are deeply excavated.

C5 is almost complete, lacking only the right prezygapophysis and the neural spine (Figs. 5, 6). The neural arch is not as anterodorsally slanted in lateral view as in more anterior cervicals. The neural spine is not preserved but its base is subquadrangular in cross-section and located on the posterior half of the neural arch, with a deep prespinal fossa located anteriorly (Figs. 5, 6). As in C4, the prezygapophysis is dorsally directed, with a sharp anterior ridge, and a well-developed bulge and triangular depression (Fig. 5). The postzygapophysis lacks a suprapostzygapophyseal lamina and bears a small circular depression anteroventral to the postzygapophyseal facet (Fig. 5).

The diapophysis of C5 is more robust than those of the more anterior cervical vertebrae, with a large and subcircular articular facet contrasting with the more anteroposteriorly elongated facets of the anterior cervicals. Similarly, the parapophysis is more elongate, laterally directed, and occupies a relatively larger proportion of the lateral surface of the centrum than in anterior cervicals (Fig. 5). The hypapophysis projects from the anterior one-third of the centrum with a straight posterior margin, lacking the posteroventral orientation of more anterior hypapophysis.

C6 only preserves the centrum and the base of the neural arch (Fig. 5). The diapophysis of C6 is robust and expands markedly at its distal tip, forming a large, subcircular articular facet. The diapophyseal process is longer and not as ventrally directed as in C5. The parapophysis and hypapophysis are similar to those of previous vertebrae although the former is dorsoventrally lower (Fig. 5).

C7 consists of the centrum and anterior region of the neural arch. The prezygapophyseal process has a well-developed prezygapophyseal bulge (Fig. 5) and a deep but dorsoventrally short triangular depression on its medial surface. The prezygapophyseal articular facets are more vertically oriented than in more anterior cervicals, forming an angle of 55 degrees with the sagittal plane. The diapophysis is more robust than in other cervicals and its articular facet is markedly expanded with respect to the rest of the diapophyseal process (Fig. 5). The parapophysis and hypapophysis are similar to those of C6, although the latter is more ventrally extended. The centrum of C7 has only moderately developed depressions on its lateral and ventral surfaces and its mediolateral midpoint constriction is less marked than in preceding cervical vertebrae.

An isolated vertebral centrum MPEF-PV 3971 is interpreted as C8, an element that is missing from MPEF-PV 1776. The parapophyseal articular facet is rounded (as in the dorsal vertebrae; see below) and located on the ventral half of the centrum, a position that is intermediate between those present in anterior dorsals and posterior-most cervicals preserved in MPEF-PV 1776. Furthermore, the position of the parapophysis is congruent with that of C8 of extant crocodylians. In contrast to the morphology of the preceding cervicals, the parapophysis of C8 is taller than long (as in the anterior dorsals). A similar anteroposteriorly short parapophysis is present in C8 of extant crocodylians, reinforcing the identification of this element. The centrum is only moderately constricted at its midpoint as in the preceding vertebra, with a well-developed, laminar hypapophysis.

Dorsal Vertebrae—Ten dorsal (D) vertebrae are preserved in MPEF-PV 1776, including two anterior dorsals and eight middle to posterior dorsals (interpreted as a continuous series from D5 to D12). These vertebrae are described in three sections representing the anterior, middle, and posterior regions.

The anterior dorsals are characterized by the presence of a dorsoventrally elongated parapophysis located at the level of the neurocentral suture (Fig. 7), as in *A. gomesii*, *Simosuchus*, *Notosuchus*, *B. albertoi*, and *Mahajangasuchus*. The parapophysis of basal crocodyliforms and neosuchians, by contrast, are subcircular or anteroposteriorly elongated. The position of the parapophyses in the anterior vertebrae of *Sebecus icaeorhinus* is congruent with those of the D2 and D3 of other taxa (*A. gomesii*,

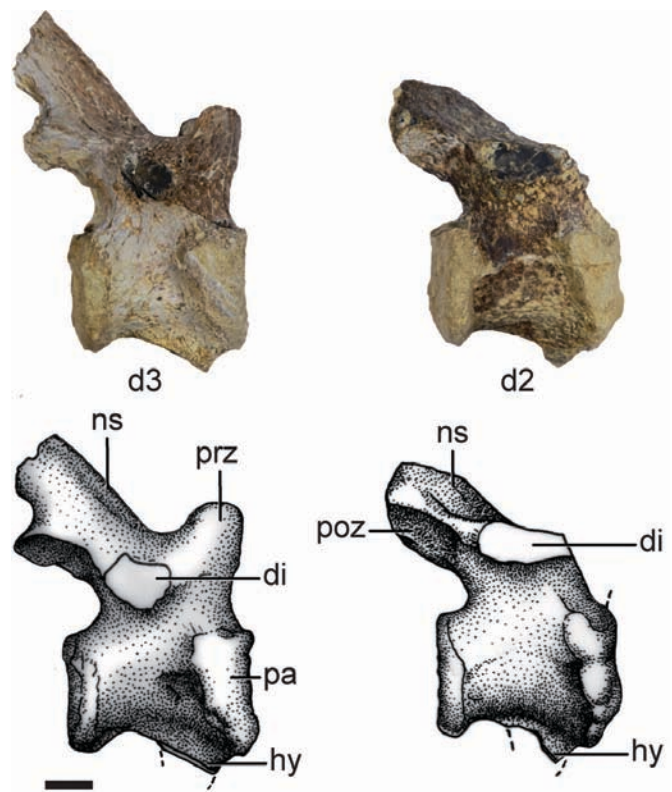


FIGURE 7. Dorsal vertebrae 1–2 of *S. icaeorhinus* (MPEF-PV 1776) in right lateral view. D1 is on the right. Scale bar equals 1 cm. (Color figure available online.)

crocodylians) and they are therefore interpreted as D2 and D3. Parts of the neural arches of the anterior dorsals are missing but their pedicles are dorsoventrally short and anteroposteriorly long in comparison with those of the cervical vertebrae. The neural spine of D3 is anteroposteriorly short, located on the posterior half of the neural arch, and directed posterodorsally forming an angle of approximately 40 degrees with the longitudinal axis (Fig. 7), as in *Mahajangasuchus*. The posterior edge of the neural spine has a mediolaterally broad medial lamina that is preserved between the postzygapophyses. Anteriorly, the dorsal surface of the neural arch has a small depression, but lacks the deep prespinal fossa of the cervical vertebrae (Fig. 8). The prezygapophyses are short and dorsally directed and their anterior surface lacks the bulge present in the cervical vertebrae. The articular facets of the prezygapophysis are flat and ovoid (transversely elongated). The postzygapophyses have an incipiently developed suprapostzygapophyseal lamina along the posterior margin of the neural spine, enclosing the medial lamina. The posteroventral surface of the postzygapophyseal process bears a curved groove that runs medially to the articular facets of the postzygapophyses (Fig. 8).

The parapophyses are subtriangular, dorsoventrally tall, and obliquely oriented, with their broad dorsal end directed posterodorsally (Fig. 7), as in *Baurusuchus*. The diapophysis is not complete but its process is anteroposteriorly short and deep, located only slightly ventral to the zygapophyses. Only the base of the hypapophysis is preserved, indicating these vertebrae had a laminar hypapophysis along the anterior one-third of the centrum (Fig. 7). The lateral surfaces of the centrum are only slightly depressed, contrasting with the highly excavated cervical centra.

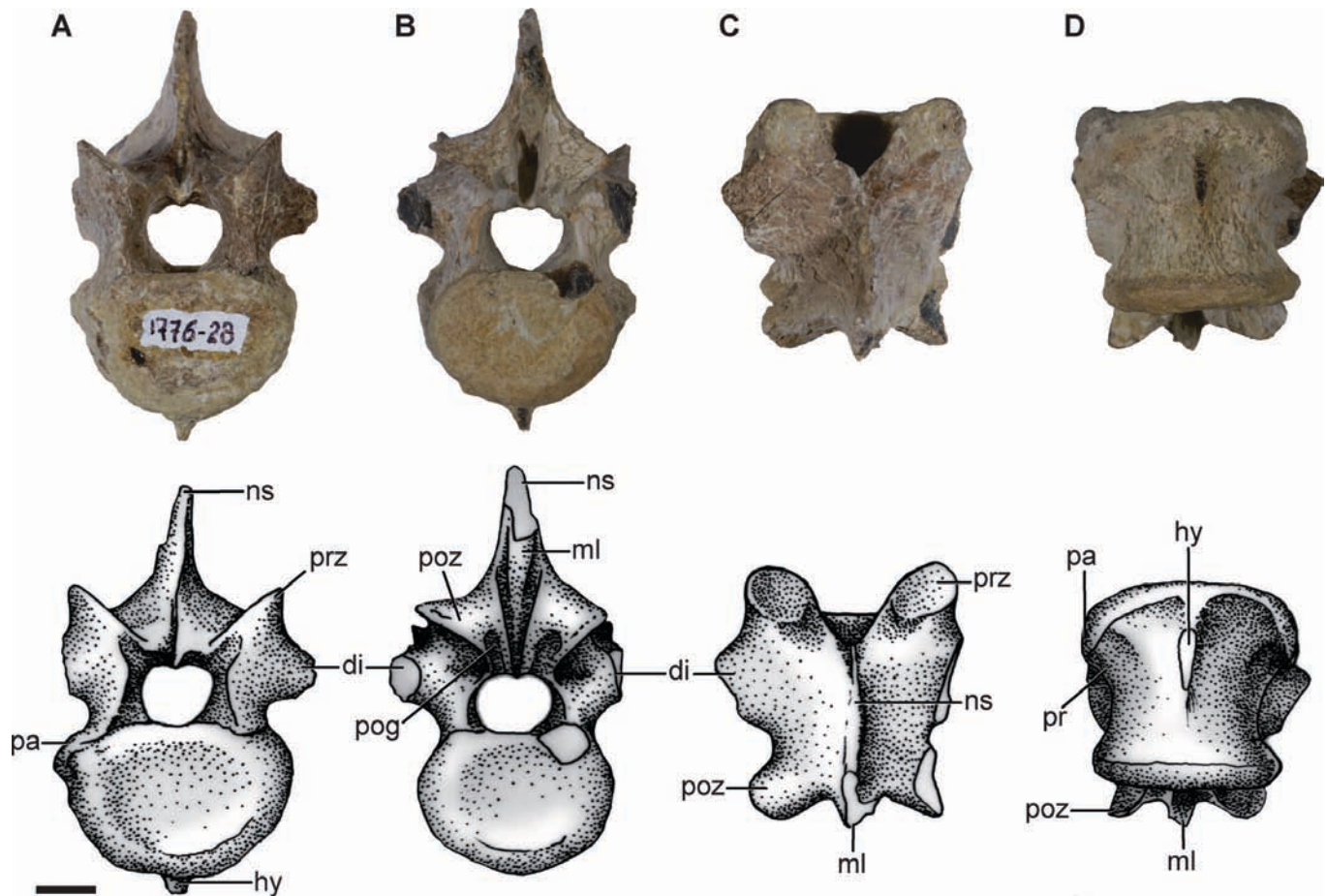


FIGURE 8. Dorsal vertebra 2 of *S. icaeorhinus* (MPEF-PV 1776) in **A**, anterior view; **B**, posterior view; **C**, dorsal view; and **D**, ventral view. Scale bar equals 1 cm. (Color figure available online.)

The middle dorsal vertebrae are characterized by the presence of a well-defined parapophysis located anteroventral to the diapophysis and a thin but well-developed parapodiapophyseal lamina (Fig. 9). The dorsal migration of the parapophysis along this series is gradual as in other non-neosuchian crocodyliforms, contrasting with the abrupt shift between D4 and D5. The parapophysis of D4 of crocodylians and some notosuchian crocodyliforms (e.g., *Baurusuchus*, *Notosuchus*) is located at the dorsoventral midpoint of the neural arch pedicles. Given that the anterior-most middle dorsal of MPEF-PV 1776 has a more dorsally located parapophysis, we interpret this series as D5 to D8.

The middle dorsals are mostly complete, with the neural arches anteroposteriorly longer than in preceding vertebrae. Only the bases of the neural spines are preserved in these vertebrae, which vary in their orientation along this series. The base of the neural spine of D5 is directed posterodorsally, as in the anterior dorsals, whereas those of D7 and D8 are vertically oriented. The anterior margin of the neural spine extends to the edge of the neural arch, where a small anteriorly open notch is present (incisura vertebralis cranialis sensu Frey, 1988; Fig. 10). The prezygapophysis in D5 is short and vertically oriented as in the anterior dorsals. In contrast, D6 to D8 have shorter prezygapophyses that are barely elevated from the dorsal surface of the neural arch (Fig. 9). The anterior surface of the prezygapophyseal process is broad and convex (Fig. 10) and lacks a prezygapophyseal bulge. The articular facets of the prezygapophyses become more transversely

elongated and more horizontally inclined along this series. The postzygapophyses increase in size and posterior projection along this series and consequently the postspinal fossa becomes increasingly deeper. The suprapostzygapophyseal laminae are absent in these vertebrae (as in *Baurusuchus*), except for D5, in which an incipient lamina is present. The postzygapophyseal groove is only present in D5 and D6 (Fig. 10). In D7 and D8 the base of the medial margins of the postzygapophyses are connected to each other by a transversely oriented lamina that forms the floor of the deep postspinal fossa.

The parapophyses of the middle dorsals are much smaller and are more laterally projecting than in the preceding vertebrae. The parapophyseal process projects ventrolaterally in D5 and gradually shifts its orientation to a lateral projection in D7 and D8. The terminal articular facets are rounded and connected to the diapophysis by a parapodiapophyseal lamina (Fig. 9). This lamina, absent in extant crocodylians, changes its orientation along this series due to the dorsal shift in the position of the parapophysis. Given the presence of the parapodiapophyseal lamina, the dorsal surface of the neural arch consists of a broad horizontal lamina bounded posteriorly by a narrow notch that separates the postzygapophysis from the posterior margin of the diapophysis (Fig. 10). The middle dorsal diapophyses are located at the level of the zygapophyses, as in most basal mesoeucrocodylians (e.g., *Baurusuchus*, *Mahajangasuchus*, *Lomasuchus*), contrasting with the more ventrally located diapophyses of neosuchians and basal

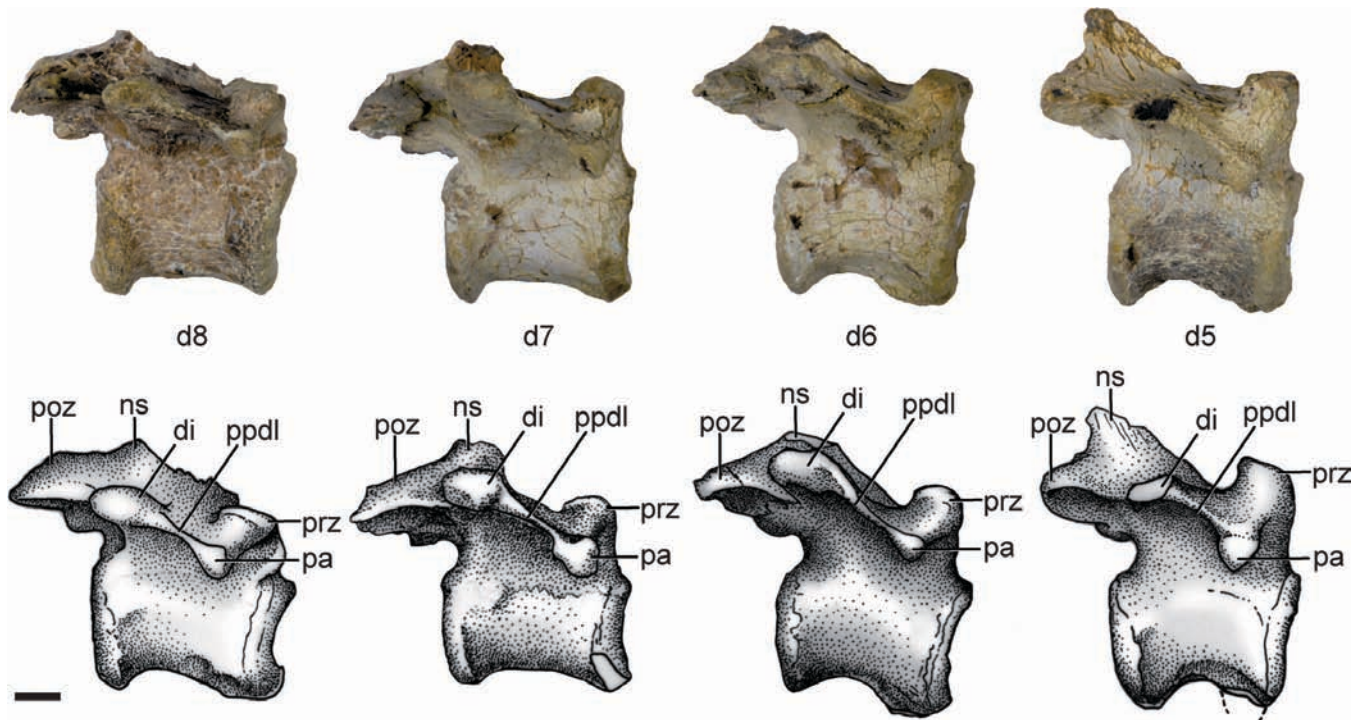


FIGURE 9. Dorsal vertebrae 5–8 of *S. icaeorhinus* (MPEF-PV 1776) in right lateral view. D5 is on the right. Scale bar equals 1 cm. (Color figure available online.)

crocodyliforms (e.g., *Gobiosuchus*, *Protosuchus*). The diapophyseal process is laminar and oriented laterodorsally in anterior view (Fig. 10). A hypapophysis is present in D5 and D6, but is completely absent in more posterior dorsals. The lateral surfaces of the centrum lack distinct depressions and are only slightly constricted at their midpoint in ventral view (Fig. 10).

The parapophyses of the posterior dorsal vertebrae are located near the level of the diapophysis, forming an anteroposte-

riorly broad transverse process (Fig. 11). Given that the anterior-most of these vertebrae possesses a parapophysis that is elevated slightly relative to that of D8, and due to the gradual dorsal shift of the parapophysis along this series, these vertebrae are identified as D9–D12.

The base of the neural spine of D9 is vertically oriented, whereas those of D10–D12 are anterodorsally oriented. The neural spines of the posterior dorsal vertebrae lack anterior and

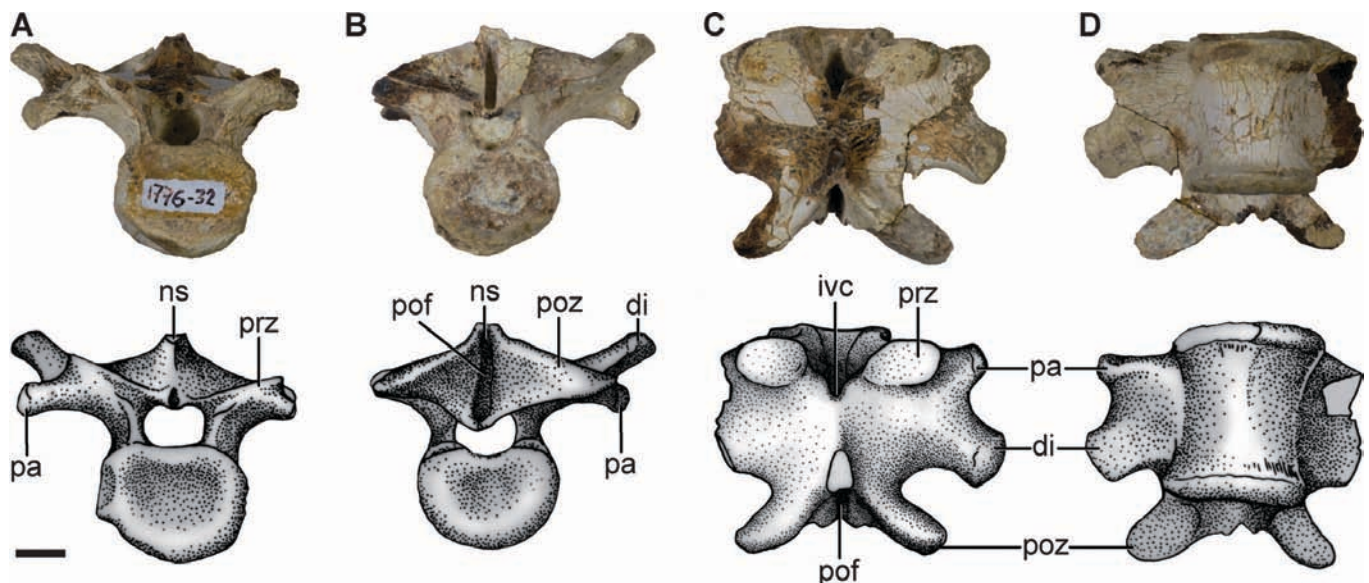


FIGURE 10. Dorsal vertebra 7 of *S. icaeorhinus* (MPEF-PV 1776) in **A**, anterior view; **B**, posterior view; **C**, dorsal view; and **D**, ventral view. Scale bar equals 1 cm. (Color figure available online.)

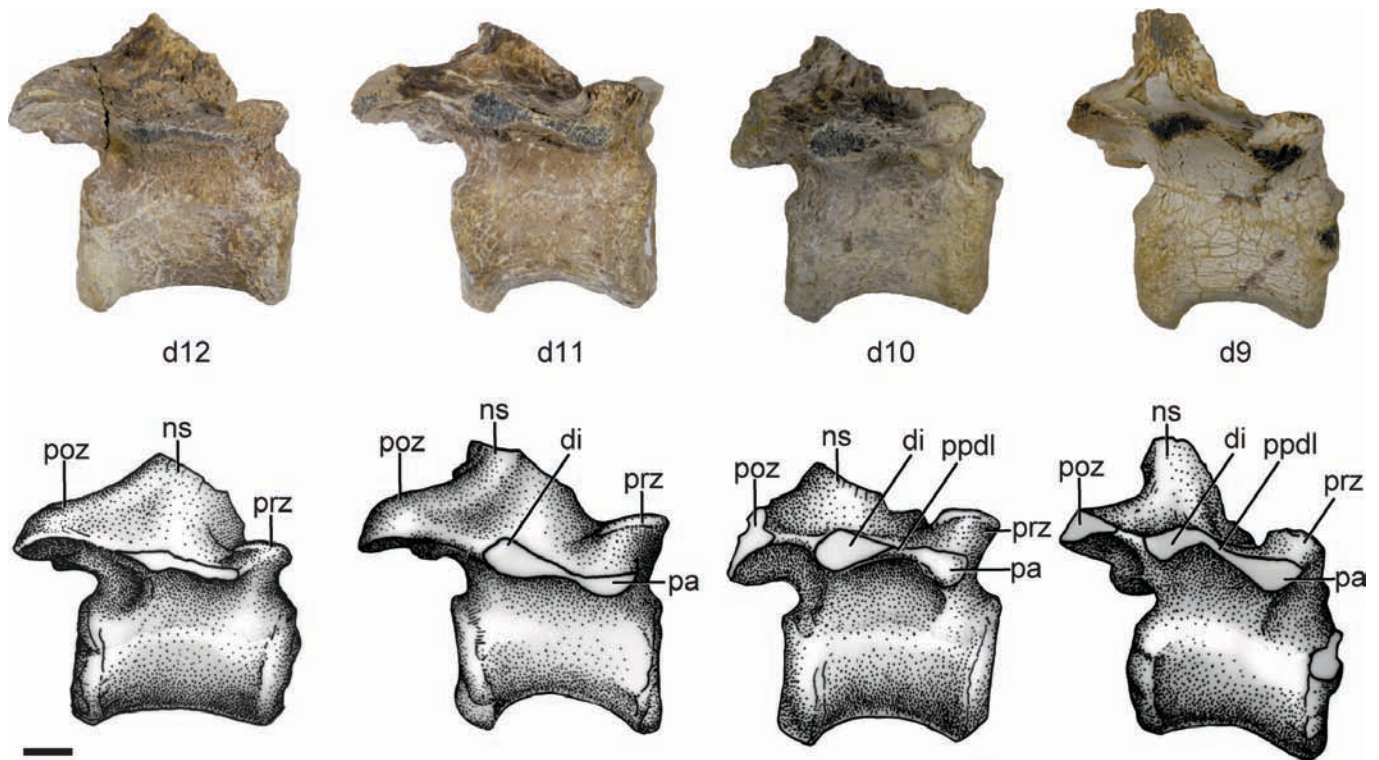


FIGURE 11. Dorsal vertebrae 9–12 of *S. icaeorhinus* (MPEF-PV 1776) in right lateral view. D9 is on the right. Scale bar equals 1 cm. (Color figure available online.)

posterior medial laminae. The anterior edge of the neural arch bears a broad concave notch, whereas in D9 the notch is narrow as in the middle dorsals. The prezygapophyses of the posterior dorsals are low, lack a prezygapophyseal bulge, and bear transversely elongated and sub-horizontal articular facets. The postzygapophyses are projected posteriorly and bear a deep postspinal fossa between them. The parapophysis of D10 has a tear drop-shaped articular facet, with the acute end pointing posteriorly. The parapodiapophyseal lamina is short and extends horizontally toward the diapophysis, though in D9 this lamina is slightly obliquely oriented (Fig. 11). The parapophyseal and diapophyseal processes are incomplete but preserved portions indicate they are sub-horizontal, laterally projecting, and level with the zygapophyses. A hypapophysis is absent in all posterior dorsals.

Sacral Vertebrae—The centrum of the first sacral vertebra of MPEF-PV 1776 is much broader and taller anteriorly than posteriorly (see Supplementary Data). The right prezygapophysis is as mediolaterally broad as in the posterior dorsals but the postzygapophyses are much smaller and do not project as far laterally. The right sacral rib is robust and dorsoventrally tall, attaching to the medial surface of the ilium at the level of the anterior margin of the acetabulum and the anterior peduncle of the ilium (see below). The dorsal portion of the sacral rib projects laterodorsally, dorsally surpassing the neural canal, as in *Araripesuchus*, but contrasting with the shallower ribs of crocodylians and thalattosuchians (e.g., *Steneosaurus*). Although only one sacral vertebra was preserved in MPEF-PV 1776, the articular facets for the sacral ribs on the ilium suggests the presence of no more than two sacral vertebrae in *S. icaeorhinus*, contrasting with the three sacrals of many notosuchians (e.g., *Notosuchus*, *Mariliaesuchus*, *Baurusuchus*). However, in *Notosuchus*, two of the three sacral vertebrae and ribs are completely fused to each other (Pol, 2005), so inferring the number of sacral vertebrae from the iliac attachment areas may be misleading.

Pectoral Girdle

Pectoral girdle elements preserved in the new specimens are represented by three partially preserved coracoids (MPEF-PV 1776, 3972).

Coracoid—The left coracoid of MPEF-PV 1776 is the most complete, preserving the proximal region and half of the shaft (Fig. 12), whereas the two coracoids of MPEF-PV 3972 only preserve their proximal ends. The external surface of the coracoid is convex but the internal surface is slightly concave. The proximal expansion of the coracoids is broad and subrectangular, bearing a coracoid foramen that is well separated from the proximal articular surface (Fig. 12A, B). This articular surface is subtriangular and divided by an oblique crest (Fig. 12C) with its apex directed anteriorly, in contrast to the more rectangular scapular articular surfaces of *Protosuchus*, *Lomasuchus*, *Notosuchus*, and baurusuchids. The glenoid facet is directed posterolaterally but lacks the expanded ventral margin that overhangs the deep ventral recess present in *A. tsangatsangana*, *Lomasuchus*, and baurusuchids. The glenoid articular surface itself is subrectangular with its main axis oriented mediolaterally. Ventromedial to the glenoid process, the coracoid bears a slightly rugose ridge that likely marks the origin of the *M. triceps longus caudalis* (Meers, 2003). The coracoid shaft is narrow, measuring only 31% of the anteroposterior length of the proximal end of the coracoid. This constriction is much more pronounced than the 40% anteroposterior ratio observed in other crocodyliforms, including *Notosuchus* (MACN-PV RN 1024), *Stratiotosuchus*, *Baurusuchus*, and crocodylians (e.g., *Caiman*).

Forelimb

The forelimb is represented by the humerus, ulna, radius, and radiale (MPEF-PV 1776), and additional fragmentary remains (MPEF-PV3972).

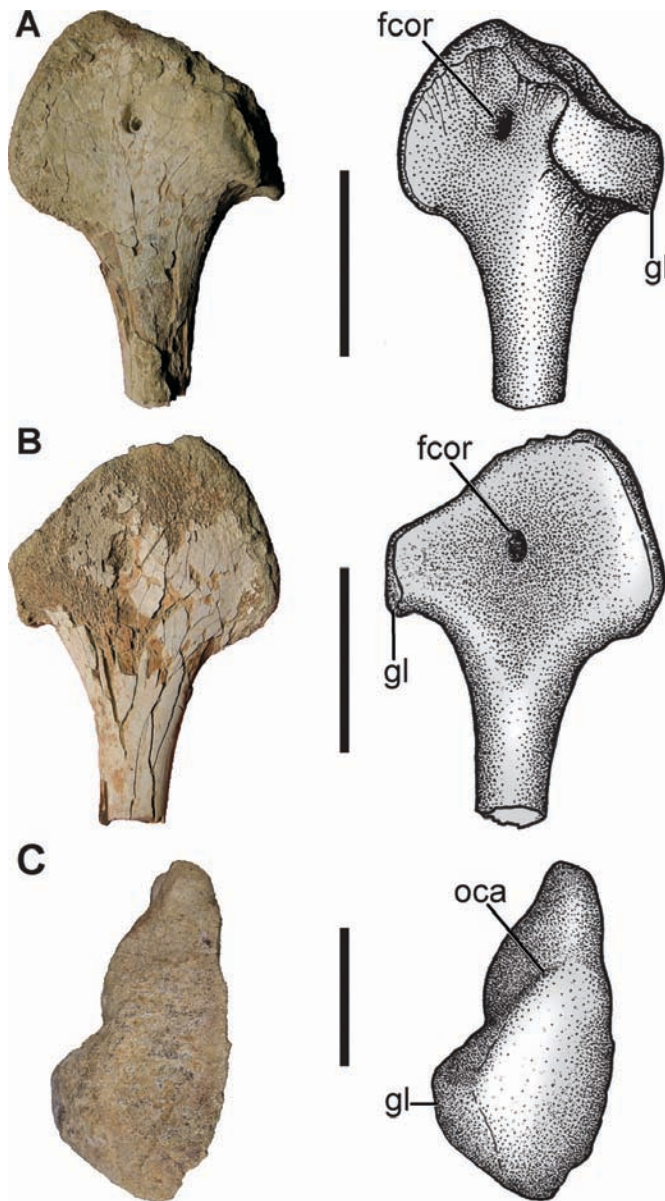


FIGURE 12. Left coracoid of *S. icaeorhinus* (MPEF-PV 1776) in **A**, lateral view; **B**, medial view; and **C**, proximal view. Scale bars equal 3 cm. (Color figure available online.)

Humerus—The humerus of *S. icaeorhinus* (Fig. 13) is more gracile and straighter in lateral view than the humerus of extant crocodylians. The humeral shaft is circular in cross-section, with its midshaft width 10% of the total humeral length, resembling the proportions of the gracile humeri of *Stratiotosuchus* (10%) and *Malawisuchus* (9%), but contrasting with the relatively more robust humeri of extant crocodylians (12–14%), *Simosuchus* (12%), and *Notosuchus* (14%). The proximal expansion is slightly arched posteriorly in medial and lateral views (Fig. 13B, D). As in most basal mesoeucrocodylians, a deep depression is located on the posterior surface of the proximal humerus (Fig. 13C) for the insertion of the *M. scapulohumeralis caudalis* (Meers, 2003). This depression is proximally limited by a posteroventral projection of the articular surface, as in other basal mesoeucrocodylians (e.g., *Notosuchus* MACN-PV RN1042, *Lomasuchus*, *Mahajangasuchus*, *Iberosuchus*, bau-

rusuchids). The internal tuberosity is poorly developed and the surface for the insertion of the glenohumeral stabilizer, the *M. subscapularis* (Meers, 2003), above the tuberosity is vertical and faces medially, as in *Chimaerasuchus*, *Iberosuchus*, and baurusuchids. In *Simosuchus*, *Lomasuchus*, and extant crocodylians, the internal tuberosity projects strongly medially and the surface for muscular insertion is obliquely oriented and exposed dorsomedially. Ventral to this tuberosity the surface of the humerus bears marked rugosities (Fig. 13D) that likely represent the origin of the *M. triceps brevis caudalis* (Meers, 2003). As in most basal mesoeucrocodylians, the proximal end of the anterior surface (Fig. 13A) has a broad, but shallow, depression for the insertion of the *M. coracobrachialis brevis ventralis* (Meers, 2003).

The deltopectoral crest (Fig. 13A) is displaced medially, leaving a slightly concave surface lateral to the crest on the anterior surface of the humerus, as in *Notosuchus*, baurusuchids, and *Iberosuchus*. In other basal mesoeucrocodylians, the proximal region of the deltopectoral crest is located at the lateral margin of the anterior surface of the humerus (e.g., *Araripesuchus*, *Simosuchus*, *Malawisuchus*, *Mahajangasuchus*, *Lomasuchus*). The deltopectoral crest deflects medially at its distal end, reaching the mediolateral midpoint of the humeral shaft, extending distally beyond the humeral proximodistal midpoint, as in baurusuchids. In *A. tsangatsangana* and *Iberosuchus*, the distal end of the deltopectoral crest is also deflected medially but does not reach the mediolateral midpoint of the shaft. The medial displacement of the proximal origin of the deltopectoral crest may have resulted in the anterior displacement of the insertion of several stabilizer muscles of the glenohumeral joint (e.g., *M. coracobrachialis brevis dorsalis*, *M. deltoideus clavicularis*, and *M. deltoideus scapularis*). As noted by Riff (2007) for *Stratiotosuchus*, the medial deflection of the deltopectoral crest in *S. icaeorhinus* may have added a protractive vectorial component to several abductor muscles (*M. deltoideus clavicularis*, *M. triceps brevis cranialis*, *M. humeroradialis*). The deltopectoral crest does not appear to have the pointed anterior tubercle for the insertion of the *M. supracoracoideus*, present in most crocodyliforms (including *Araripesuchus*, *Lomasuchus*, *Mahajangasuchus*). A low deltopectoral crest apex is also present in *Notosuchus*, *Simosuchus*, and baurusuchids.

Posterolateral to the proximal origin of the deltopectoral crest are two conspicuous tuberosities (Fig. 13B). The dorsomedial tuberosity likely corresponds topographically with the insertion of the *M. coracobrachialis brevis dorsalis* and the ventrolateral one with the insertion of the *M. deltoideus scapularis* (Meers, 2003), as in *Notosuchus* and baurusuchids. This contrasts with the well-developed scar present in extant crocodylians (Meers, 2003), *Araripesuchus*, *Simosuchus*, *Mahajangasuchus*, and *Iberosuchus*. In extant crocodylians, the scar is placed distal to a well-developed ridge that runs from the posterolateral border of the proximal humerus, a set of features that are also present in *Mahajangasuchus* and *Iberosuchus*, but absent in *S. icaeorhinus*, baurusuchids, and *Notosuchus*.

The distal humerus consists of two distinct hemicondyles. The medial hemicondyle is distally projected and is about one-half of the width of the lateral hemicondyle. Both hemicondyles extend onto the anterior surface of the humerus, forming a proximally exposed shelf that is bounded by two well-developed anterior supracondylar ridges (Fig. 13B, D), as in *Iberosuchus*. A similar shelf is also present in other basal mesoeucrocodylians (e.g., baurusuchids, *A. tsangatsangana*, *Mahajangasuchus*,

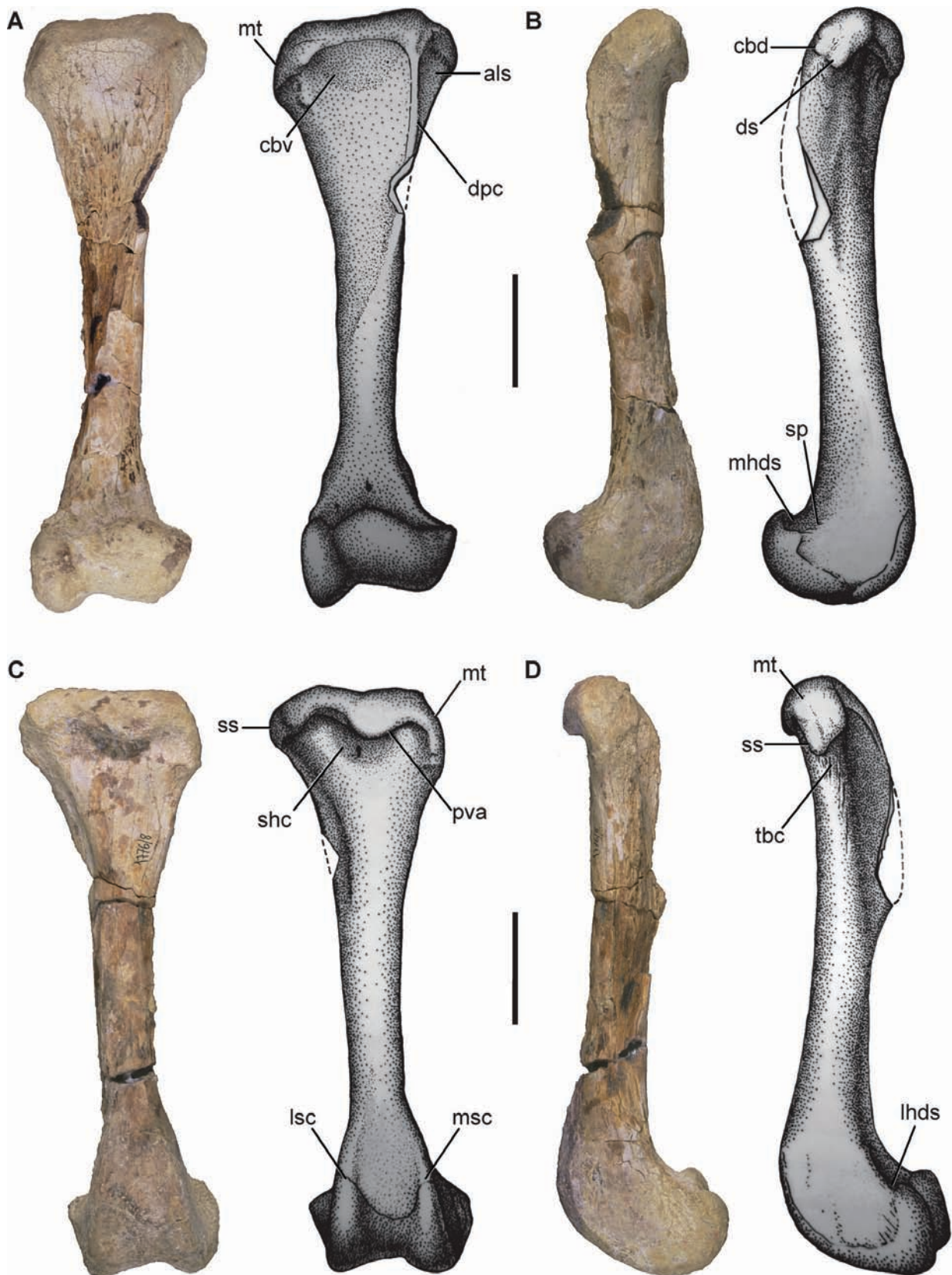


FIGURE 13. Left humerus of *S. icaeorhinus* (MPEF-PV 1776) in **A**, anterior view; **B**, lateral view; **C**, posterior view; and **D**, medial view. Scale bars equal 3 cm. (Color figure available online.)

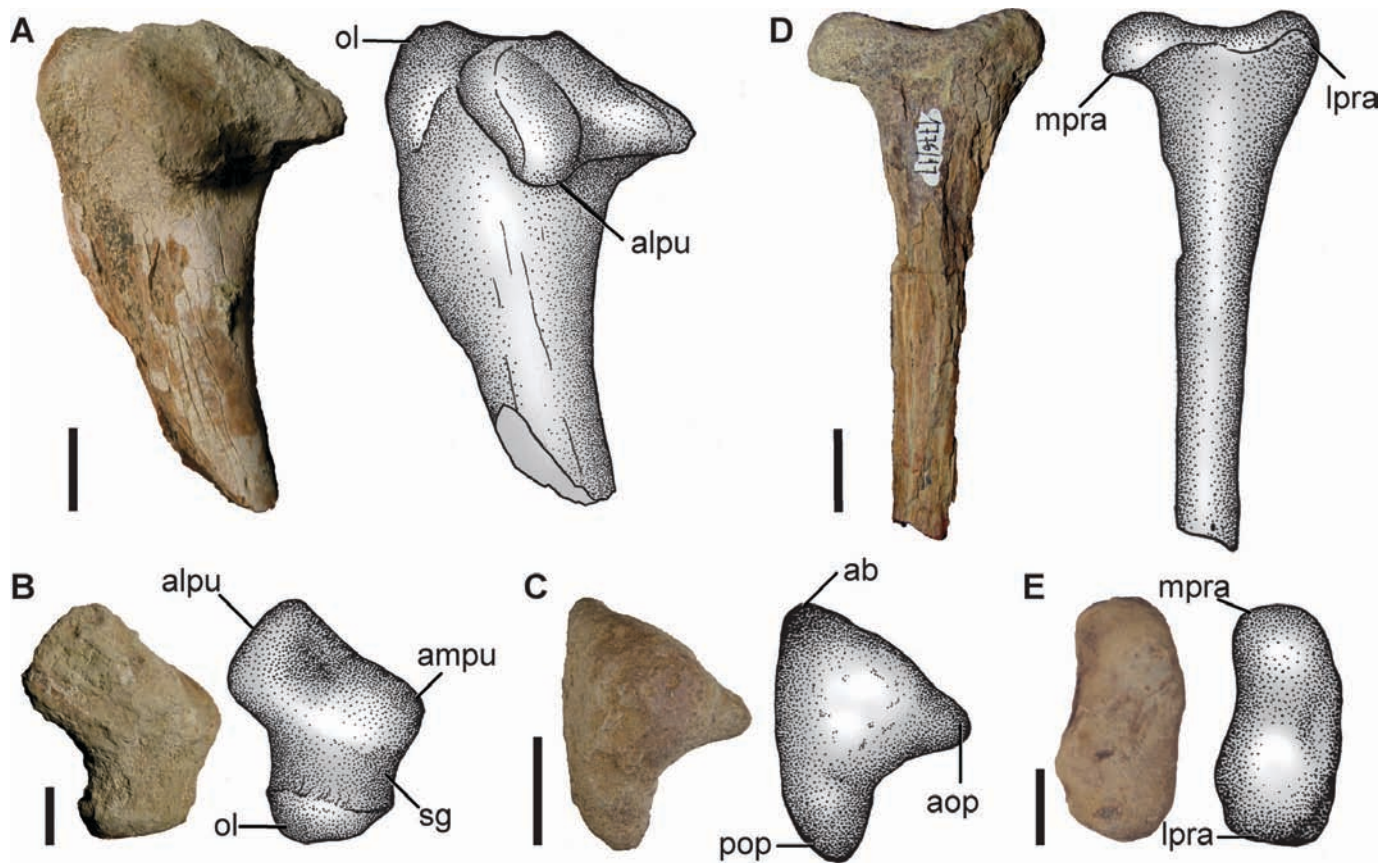


FIGURE 14. Ulna and radius of *S. icaeorhinus* (MPEF-PV 1776). Left ulna in A, lateral; B, proximal; and C, distal views; left radius in D, anterior; and E, proximal views. Scale bars equal 1 cm. (Color figure available online.)

Lomasuchus), although in these forms the shelf is not as mediolaterally extensive or bounded by supracondylar ridges. The posterior supracondylar ridges are also well developed, with the lateral ridge more prominent and more proximally extended (Fig. 13C), as in *Stratiotosuchus*, *Lomasuchus*, *Mahajangasuchus*, and *Iberosuchus*. In other basal mesoeucrocodylians (e.g., *Notosuchus*, *Araripesuchus*, *Uruguaysuchus*; Rusconi, 1933), the medial ridge is more prominently developed. Together, the posterior supracondylar ridges enclose an elongated, trough-shaped, and strongly concave depression in distal view, as in *Stratiotosuchus* and *Lomasuchus*. In contrast, extant crocodylians and *Notosuchus* have a much more shallow depression that is less extended proximally. The lateral and medial distal surfaces of the humerus are flat, as in other basal mesoeucrocodylians. A short crest on the lateral surface of the distal humerus (Fig. 13B) likely marks the origin of the *M. supinator*, as in extant crocodylians (Meers, 2003).

Ulna—The ulnae of MPEF-PV 1776 (Fig. 14) both preserve their proximal and distal regions. The proximal end (Fig. 14A, B) has three processes: a well-developed olecranon directed posteriorly, an anteromedial process, and an anterolateral process (for articulation with the radius). The proximal surface of the ulna (Fig. 14B) has an elevated central area that separates the concave anterolateral and anteromedial processes. The olecranon is located posterior to this elevated area, separated from it by a shallow groove (Fig. 14B). This morphology closely resembles that of *Notosuchus*, *Mahajangasuchus*, *Baurusuchus*, and *Stratiotosuchus*. In extant crocodylians, the three processes of the proximal surface of the ulna are weakly developed. The distal

end of the ulna has a complex articular surface consisting of two oblique processes (anteriorly and posteriorly directed) and an anterolateral rugose bulge (Fig. 14C). This morphology is also present in most basal mesoeucrocodylians (e.g., *Notosuchus*, *Mahajangasuchus*, baurusuchids), but contrasts with the condition of extant crocodylians in which these processes are weakly developed (Pol, 2005).

Radius—The most complete radius preserves the proximal end and part of the shaft (Fig. 14D, E). The proximal end has two processes: a mediolaterally broad and medially projecting process and a smaller lateral process that is slightly posteriorly curved (Fig. 14E). Both processes are separated by a shallow concavity on the proximal surface of the radius and have roughly the same proximal projection, as in extant crocodylians. In contrast, the lateral process of the radius is more proximally projected in *Notosuchus*, *Stratiotosuchus*, and *Baurusuchus*. The radial shaft of the radius is ovoid in cross-section.

Radiale—The proximal portion of the radiale is preserved in MPEF-PV 1776 (Fig. 15). The proximomedial corner bears a distinct acute process (Fig. 15A), absent in other crocodyliforms. The proximal articular surface is crescentic and divided in two regions: a large, subquadrangular lateral surface and a narrow subrectangular medial surface that extends onto the proximal surface of the proximomedial process of the radiale.

The radiale has an oblique, proximodistally elongate, and posteriorly directed process for articulation with the ulna and ulnare (Fig. 15B, C). Both the length and orientation of this process are unique to *S. icaeorhinus*. The posterior surface of this process has two distinct articular surfaces divided by an

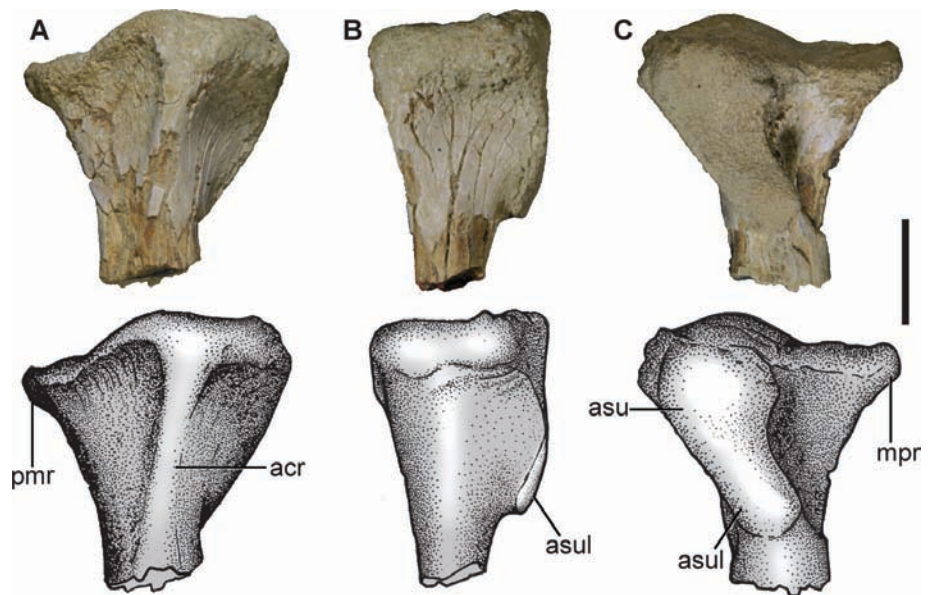


FIGURE 15. Radiale of *S. icaeorhinus* (MPEF-PV 1776) in **A**, anterior view; **B**, medial view; and **C**, posterior view. Scale bar equals 1 cm. (Color figure available online.)

oblique and mediolaterally oriented crest. The most proximal of these articular surfaces occupies most of this process and likely contacted the ulna. The smaller distally located articular surface faces posteriorly and slightly laterally, and likely contacted the ulnare (Fig. 15B). A distinct articular surface for the ulnare is present in other basal mesoeucrocodylians, but is absent in basal crocodylomorphs (e.g., *Protosuchus*, *Terrestriusuchus*, *Dibotosuchus*) and Crocodylia. Medial to the posterolateral process, the posterior surface of the radiale is strongly concave, where the *M. flexor digiti quinti pars superficialis et profundus* originates in extant crocodylians (Meers, 2003). The anterior surface of the radiale has a well-developed proximodistal ridge (Fig. 15A), as in *Notosuchus*, *baurusuchids*, and *Mahajangasuchus*.

Pelvic Girdle

The pelvic girdle of *Sebecus icaeorhinus* is known only in MPEF-PV 1776, which includes both complete ilia, the complete right ischium, and a proximal portion of the left ischium.

Ilium—Both ilia are well preserved, although the acetabular region of the right ilium is slightly damaged. The ilium is antero-posteriorly long, mostly because of its long postacetabular process, accounting for approximately 45% of the total iliac length (Fig. 16). This relationship contrasts with that of several basal mesoeucrocodylians, which have a relatively small process (e.g., *A. tsangatsangana* [38%], *Mahajangasuchus* [39%], *B. albertoi* [34%]).

In dorsal view the postacetabular process is slightly concave and laterally deflected (Fig. 16B). In lateral view, the postacetabular process tapers posteriorly, with its posterior end rounded and dorsoventrally short (Fig. 16A). The posterior end of the postacetabular process in all other basal mesoeucrocodylians is dorsoventrally taller (e.g., *Notosuchus*, *Araripesuchus*, *Baurusuchus*, *Mahajangasuchus*).

The ventral border of the postacetabular process is mediolaterally broad, straight, and posteriorly directed (Fig. 16C). A similarly oriented ventral margin of the postacetabular process is also present in most basal mesoeucrocodylians and the basal crocodyliform *P. richardsoni*, whereas in other crocodylomorphs (including extant crocodylians) the ventral margin is posterodorsally oriented (Pol, 2005). The ventral border of the postacetabular process of *Sebecus* is located ventral to the

dorsal edge of the acetabulum, a feature also found in most basal mesoeucrocodylians (e.g., *Notosuchus*, *Araripesuchus*, *Mahajangasuchus*), but not in other crocodyliforms where the ventral margin of the postacetabular process is approximately at the same level as the acetabular roof. The dorsal margin of the postacetabular process is directed posteroventrally and has short striae oriented obliquely to its dorsal border, likely related to the origins of the pelvic musculature (e.g., *M. iliobtibialis* pars 3; Romer, 1923). Except for the dorsal margin, the lateral surface of the postacetabular process is smooth with a slightly rugose concavity related to the origin of the *M. iliofemoralis* (Romer, 1923).

The preacetabular process of *S. icaeorhinus* is very short in comparison to the postacetabular process, as in most mesoeucrocodylians. However, this process is comparatively longer (8% of the total length) than in other basal mesoeucrocodylians (e.g., *A. tsangatsangana* [3.7%], *Mahajangasuchus* [3%]), and more similar to the proportions of extant crocodylians (e.g., *C. latirostris* MPEF-AC 205 [9%]). The anterior tip of the preacetabular process of *S. icaeorhinus* exceeds the anterior extent of the pubic peduncle, as in *A. gomesii* and some crocodylians (e.g., *C. latirostris*), but differing from the condition of *Notosuchus* (Fiorelli, 2005), *A. tsangatsangana*, *Mahajangasuchus*, and other crocodylians (e.g., *Alligator*; Mook, 1921; Turner, 2006). The anterior projection of the preacetabular process in *S. icaeorhinus* (and *A. gomesii*) is related not only to its length but also to the vertical orientation of the pubic peduncle, which is more anteriorly projected in other basal mesoeucrocodylians.

The ilium of *S. icaeorhinus* lacks the sharp iliac blade separated from the supracetabular crest present in most crocodyliforms. The dorsal edge of the ilium is mediolaterally broad dorsal to the acetabulum and over the anterior region of postacetabular process, where it narrows markedly (Fig. 16B). At the posterior tip of the postacetabular process, however, the dorsal surface of the ilium widens slightly. At the level of the acetabulum, the dorsal surface of the ilium projects laterally forming an extensive and rugose supracetabular crest and creating a deep horizontal acetabular roof (Fig. 16D). The dorsoventrally tall rugose surface above the acetabulum faces dorsolaterally and likely served as the insertion of the *M. iliobtibialis* 1 and 2 (Romer, 1923; Turner, 2006). Given the extensive lateral projection of the supracetabular crest and the laterally concave postacetabular process, the ilium has a sigmoid profile in dorsal view (Fig. 16B). A similar

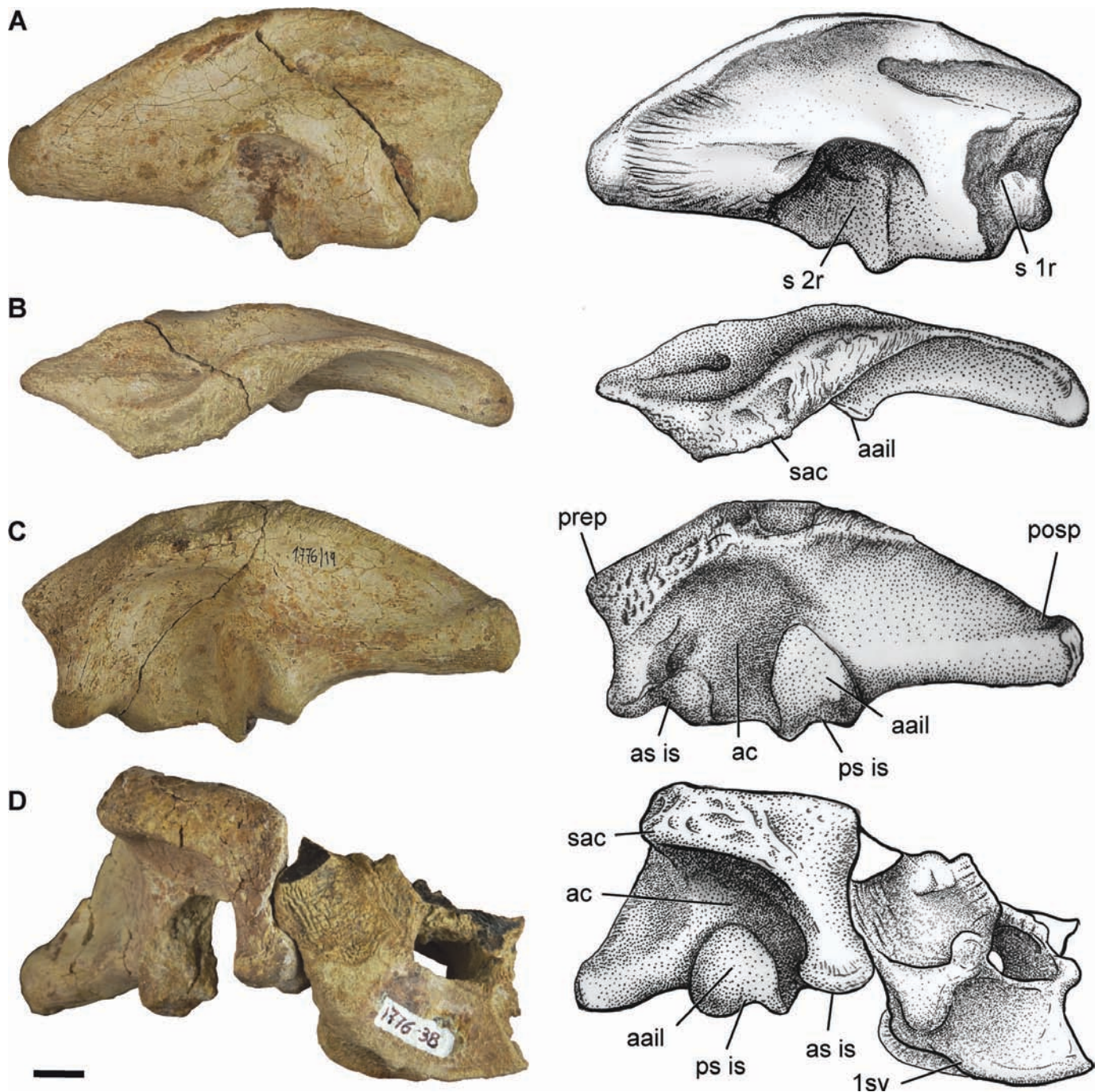


FIGURE 16. Left ilium of *S. icaeorhinus* (MPEF-PV 1776), in **A**, medial view; **B**, dorsal view; **C**, lateral view; and **D**, anterior view in articulation with first sacral vertebrae. Scale bar equals 1 cm. (Color figure available online.)

rugose, dorsoventrally thick, and horizontally oriented supracetabular crest is also present in *Notosuchus* and baurusuchids. Other basal mesoeucrocodylians (e.g., *A. tsangatsangana*, *A. gomesii*, *Mahajangasuchus*) and basal crocodyliforms (e.g., *Protosuchus* UCMP 34634) have a broad rugose surface above the acetabulum, but the supracetabular crest is not as laterally deflected and the roof of the acetabulum is not horizontally oriented. Neosuchians have a significantly reduced supracetabular crest that is not as laterally projected as in basal mesoeucrocodylians and basal crocodyliforms. The ventral margin of

the acetabulum is notched, indicating a slight perforation of the acetabulum, as in other crocodyliforms. The anterior end of the acetabulum is dorsoventrally short and well separated from the anterodorsal corner of the ilium by a wide anterolaterally facing surface.

The anterior (pubic) and posterior (ischial) peduncles each occupy approximately one-third of the ventral margin of the acetabulum. The ventral margin of both peduncles is incised by a well-developed notch (Fig. 16C). The notch on the anterior (pubic) peduncle is, however, not as deep and acute as that of

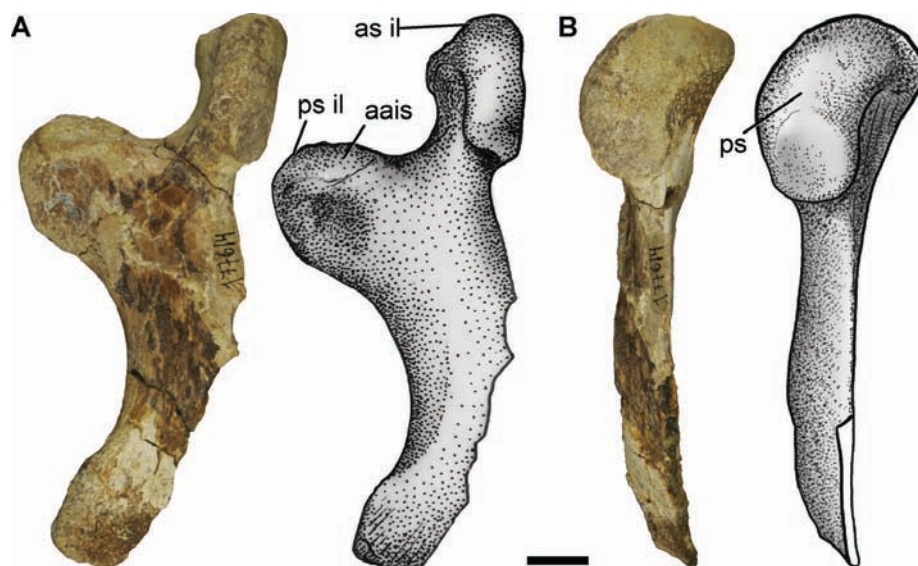


FIGURE 17. Right ischium of *S. icaeorhinus* (MPEF-PV 1776), in **A**, lateral view; and **B**, anterior view. Scale bar equals 1 cm. (Color figure available online.)

Mahajangasuchus and *Lomasuchus*. The notch on the posterior (ischial) peduncle of *S. icaeorhinus* is as well developed as that of the anterior (pubic) peduncle. Dorsal to the posterior (ischial) peduncle, the ilium of *S. icaeorhinus* has a flat anterolaterally facing surface that extends dorsally into the acetabulum, resembling the antitrochanter of theropod dinosaurs (Hutchinson, 2001a; Novas, 1993). This surface is as anteroposteriorly wide as the total articular facet of the posterior (ischial) peduncle and reaches the dorsoventral midpoint of the acetabulum (Fig. 16D), being slightly taller than anteroposteriorly wide. When the ilium and ischium are in articulation, the antitrochanter is continuous with a similar but smaller surface on the proximal region of the ischium. The presence of an iliac antitrochanter has not been frequently mentioned but a similar facet is also present in many basal mesoeucrocodylians (e.g., *A. gomesii*, *A. tsangatsangana*, *Mahajangasuchus*, *B. albertoi*, *Chimaerasuchus*). Other taxa have only a weakly developed antitrochanter that is also with flat and smooth surfaced, but usually dorsoventrally shorter than anteroposteriorly long (e.g., *Notosuchus* and extant crocodylians).

The medial surface of the ilium has two well-defined areas for the attachment of sacral ribs. The articular surface for the first sacral occupies slightly less than the anterior half of the medial acetabular wall, extending to the level of the anterior tip of the preacetabular process (Fig. 16A, D). This articular surface appears to be as dorsoventrally tall as anteroposteriorly long, contrasting with the condition present in extant crocodylians in which the articular surface is longer than tall. The articular surface for the attachment of the second sacral rib is larger than the articular surface for the first sacral rib, extending over the posterior region of the medial wall of acetabulum and the anterior portion of the postacetabular process. Therefore, the posterior postacetabular process is free of sacral attachment and would have extended over the lateral surface of the anterior caudals. This pattern of sacral attachment contrasts with the condition in other basal mesoeucrocodylians (*A. tsangatsangana*, *A. gomesii*, *Mahajangasuchus*) and extant crocodylians, in which the contact for the second sacral rib almost reaches the posterior end of the postacetabular process. The anterior and posterior sacral rib attachments of *S. icaeorhinus* are separated by a smooth non-articular region.

Ischium—The proximal region of the ischium has two well-developed processes for the anterior (pubic) and posterior (ischial) peduncles of the ilium separated by a deep and rounded

notch that forms the ventral portion of the perforated acetabulum (Fig. 17A) as in other basal mesoeucrocodylians (e.g., *Chimaerasuchus*, *Araripesuchus*, and *Mahajangasuchus*). The anterior process bears two distinct articular surfaces, one located on its dorsal surface for the anterior (pubic) peduncle of the ilium and another located on its anterior surface for its contact with the proximal pubis. Therefore, the ischium of *Sebecus* formed the entire ventral margin of the acetabulum and excluded the pubis from the acetabulum, as in all mesoeucrocodylians (Clark, 1994). The anterior process of the ischium is dorsoventrally taller than the posterior process. In anterior view, the anterior process is subrectangular in outline (Fig. 17). The articular facet for the pubis is kidney-shaped with a convex lateral edge, and a concave medial edge, with its major axis directed proximodistally. The articular facet for the pubis faces anteroventrally and is slightly medially deflected when it is articulated with the ilium.

The posterior process of the ischium has a distinct dorso-laterally facing surface continuous with the flat surface of the iliac antitrochanter (Fig. 17A). An ischial antitrochanter is also present in other crocodyliforms (e.g., *Chimaerasuchus*, *A. gomesii*, *Caiman latirostris*), although its shape and orientation varies across taxa. The articular facet for the posterior (ischial) peduncle of the ilium is flat and located posterior to the ischial antitrochanter (Fig. 17A). It faces posterodorsally and slightly laterally, with a triangular outline that tapers medially. The posterior edge of the posterior process of the ischium is large and semicircular in lateral view and merges smoothly with the posterior margin of the ischial shaft (Fig. 17A). The highly convex shape of the posteroventral margin of the posterior process of the ischium differs from the straight or slightly convex profile of other basal mesoeucrocodylians (e.g., *Stratiotosuchus*, *Chimaerasuchus*, *A. gomesii*) but resembles the morphology of extant crocodylians (e.g., *Caiman latirostris*).

The ischium of *S. icaeorhinus* lacks a well-developed ischial tuberosity, although it has a minute pointed process at the posterodistal angle of the posterior ischial process and a broad concave surface that extends on the lateral surface of this process (Fig. 17A). These structures may represent the site of origin of the *M. flexor tibialis internus* 3 (FTI3) and/or the ilio-ischial fascia similar to the ischial tuberosity of extant crocodylians (Hutchinson, 2001a).

The ischial blade is incomplete and most of the anterior margin is not preserved in MPEF-PV 1776. The proximodistal length

of the ischium from the ventral acetabulum margin to the ischial distal end is relatively short (35% of the femoral length) in comparison with other crocodyliforms. The posterior margin of the ischial shaft is markedly concave and slightly deflected medially along its shaft (Fig. 17).

Hind Limb

The hind limb of *S. icaeorhinus* is represented by two complete femora, one complete tibia, five astragali, three calcanea, and two distal tarsal 4. These pertain to multiple specimens, though the hind limb elements of MPEF-PV 1776 are the most complete.

Femur—The femur has a slight sigmoid curvature in medial and lateral views (Fig. 18A, E), resembling the condition of *A. tsangatsangana* and *Iberosuchus*. The curvature of the femur, however, is less pronounced than in the femora of *Notosuchus* (MUC-PV 900), *A. gomesii*, and extant crocodylians, and the highly sigmoid femur of *Mahajangasuchus*. The femoral head lacks a distinct femoral neck and has its major axis (from the greater trochanter to the internal part of the proximal articular surface) set at a lesser angle with respect to the transverse axis of the distal condyles than in *Mahajangasuchus* or crocodylians.

Posterolaterally on the proximal end of the femur, there is a blunt and proximodistally short greater trochanter (Fig. 18). The lateral margin of the greater trochanter consists of a faintly developed ridge that fails to reach the level of the fourth trochanter, as in *Iberosuchus* and *Mahajangasuchus*. Most other crocodyliforms (*A. gomesii*, *A. tsangatsangana*, *Notosuchus* [MUC-PV 900], *Stratiotosuchus*) have a dorsoventrally extensive trochanter, limited laterally by a sharp and well-developed ridge that serves as the insertion for the M. puboischiofemorales externus in extant crocodylians (PIFE; Hutchinson, 2001b). The distal surface for insertion of the PIFE in *S. icaeorhinus* is flat, as in extant crocodylians and *Iberosuchus*, whereas this surface is concave in other mesoeucrocodylians (e.g., *A. tsangatsangana*, *Notosuchus*, *Stratiotosuchus*). The medial edge of the greater trochanter forms a prominent and sharp longitudinal crest (Fig. 18A, B, E), as in *Iberosuchus*. This crest is much less prominent, and sometimes more distally located, in other basal mesoeucrocodylians (e.g., *Mahajangasuchus*, *Stratiotosuchus*, *Baurusuchus*, *Notosuchus*) and crocodylians.

The fourth trochanter consists of a poorly developed low bump and extends distally approximately 25–30% of the femoral length from the proximal end of the femur (Fig. 18A). The anterior surface of the fourth trochanter bears a shallow broad depression (Fig. 18A) that correlates with the insertion of two muscles in extant crocodylians. The posterior region of this depression serves as the area of insertion for the M. caudifemoralis longus (CFL), whereas the anterior region serves as the area of insertion for the M. puboischiofemorales internus 1 (PIFI1) (Hutchinson, 2001b; Carrano and Hutchinson, 2002). Both the trochanter and the anterior depression are smooth, contrasting with the rugose surface in other crocodyliforms (e.g., *Araripesuchus*, *Mahajangasuchus*, *Iberosuchus*, *Notosuchus*, baurusuchids, crocodylians). The morphology of the insertion area of PIFI1 is markedly different from that of other basal mesoeucrocodylians (except for *Iberosuchus*), in which the depression is deeper and its anterior border extends as a pronounced flange with a concave proximal margin (e.g., *Araripesuchus*, *Notosuchus*, *Simosuchus*, *Mahajangasuchus*). Baurusuchids also have this flange, although it is slightly less well developed than in the above-mentioned taxa. The absence of this flange in *S. icaeorhinus* on the proximal region of the femur results in a nearly straight anterior border in lateral view (Fig. 18F), as in basal crocodyliforms and neosuchians.

The shaft of the femur is smooth and largely lacks scars for muscular insertions, except for a faintly developed linea intermuscularis caudalis (Hutchinson, 2001b) that extends from the

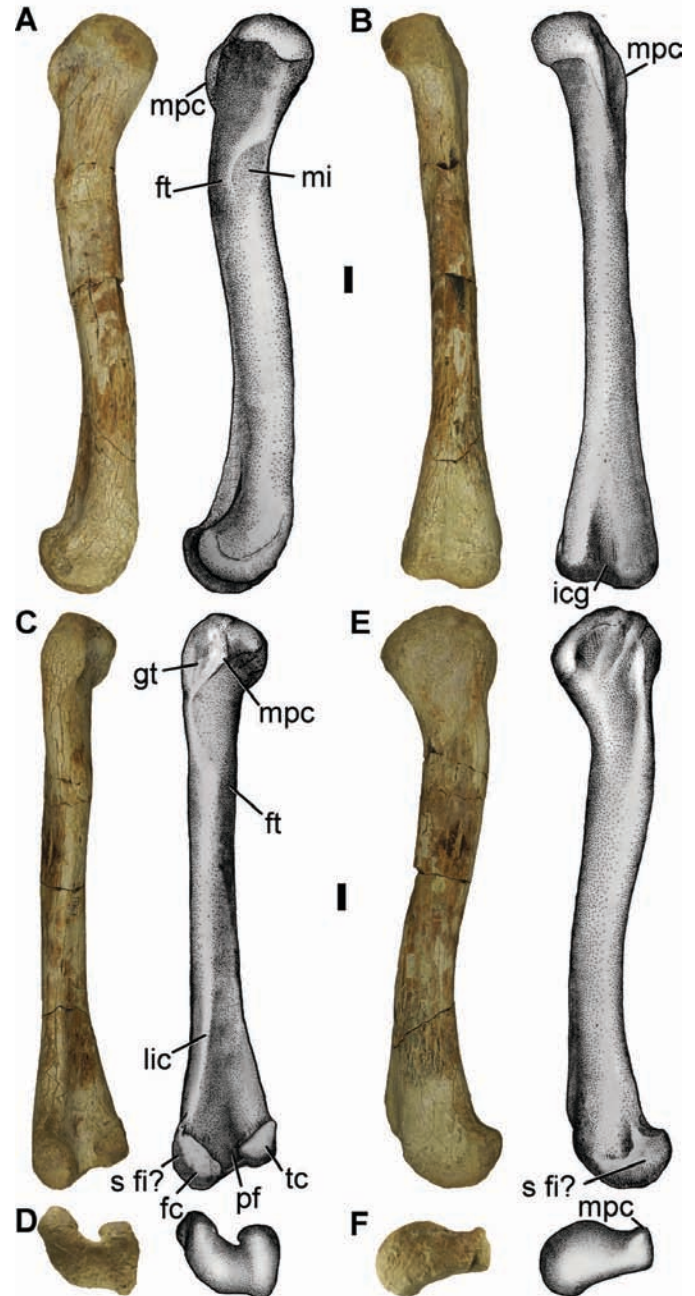


FIGURE 18. Left femur of *S. icaeorhinus* (MPEF-PV 1776), in **A**, medial view; **B**, anterior view; **C**, posterior view; **D**, distal view; **E**, lateral view; and **F**, proximal view. Scale bars equal 1 cm. (Color figure available online.)

fourth trochanter to the fibular condyle. The two distal condyles are well developed in *S. icaeorhinus* and the lateromedial width of the condylar region is more than twice the midpoint width of the shaft (Fig. 18B). The tibial condyle is anteroposteriorly shorter and mediolaterally narrower than the fibular condyle. The articular surface of the fibular condyle is semicircular, with a relatively constant lateromedial width, whereas the articular surface of the tibial condyle tapers anteriorly (Fig. 18D). The fibular condyle also projects distally beyond the level of the tibial condyle (Fig. 18C), but not to the extent observed in *Simosuchus*.

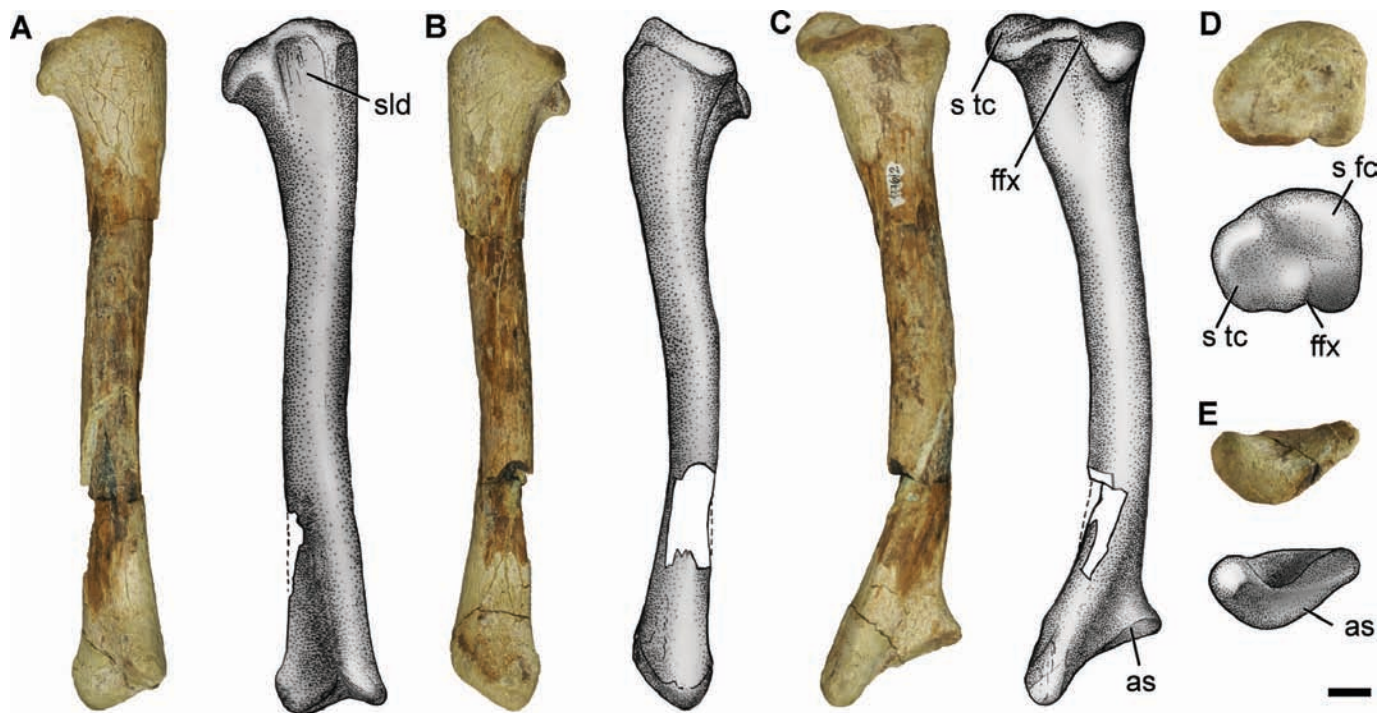


FIGURE 19. Right tibia of *S. icaeorhinus* (MPEF-PV 1776), in **A**, lateral view; **B**, medial view; **C**, posterior view; **D**, proximal view; and **E**, distal view. Scale bar equals 1 cm. (Color figure available online.)

The posterolateral corner of the articular surface of the fibular condyle bears a flat facet for the contact with the fibula (Fig. 18C, D), as in most crocodyliforms.

Distally, the anterior surface of the femur lacks a well-developed lateral supracondylar ridge such that the anterior surface of femur is only slightly concave and continuous with the lateral surface of the femur (Fig. 18B), as in *Iberosuchus*, *Notosuchus*, and *Stratiotosuchus*. The medial supracondylar ridge of the anterior surface is well developed. Posteriorly, both distal condyles are separated by a deep popliteal fossa (Fig. 18C), as in most mesoeucrocodylians. The posterior supracondylar ridge proximal to the fibular condyle forms the distal section of the linea intermuscularis caudalis. The tibial condyle lacks a well-defined supracondylar ridge on the posterior surface of the femur.

Tibia—The tibia of *S. icaeorhinus* is 77% the length of the femur (see Supplementary Data), differing from the relatively shorter tibia of baurusuchids (71–73%) and the elongated tibia of *A. tsangatsangana* (82%).

The proximal articular region of the tibia has two well-defined facets for contact with the tibial and fibular distal condyles of the femur (Fig. 19D). The proximally elevated articular facet for the tibial condyle of the femur is approximately twice as broad as the lateral articular surface along the posterior margin. This difference in the relative breadth of the posterior region of the articular facets is more notably developed in *S. icaeorhinus* than in other crocodyliforms (e.g., *Stratiotosuchus*, *A. tsangatsangana*, Crocodylia). The medial articular facet for the tibial condyle is semicircular in proximal view with its posterior region mediolaterally broader than the anterior region. This surface is weakly concave with a pronounced deflection towards the posteromedial corner (Fig. 19E). The lateral articular facet is subtriangular in proximal view, with its apex directed posteriorly (Fig. 19D). The broad anterior region of the lateral articular facet is slightly convex anteriorly and is medially bordered by the elevated medial

articular facet of the tibia. The posterior tip of the lateral articular facet is distally deflected and faces posteriorly and proximally (Fig. 19D). The posterior margins of both proximal articular facets of the tibia are separated by a small notch (fossa flexoria; Hutchinson, 2002). In proximal view, the fossa flexoria of *S. icaeorhinus* is less prominent than those of *A. tsangatsangana* or *Stratiotosuchus*, but deeper than those of *Mahajangasuchus* and *Iberosuchus*. Proximally, an anteroposteriorly centered shallow depression (Fig. 19A) is present on the lateral surface of tibia, similar to the depression located just anterior to the articulation for the fibula in crocodylians (e.g., *Caiman*). This depression fails to reach the proximal surface of the tibia and therefore is only visible in lateral view, thus contrasting with the notch formed by this depression on the lateral margin of the proximal surface of the tibia (posterior to the cnemial crest) in *Caiman*.

The preserved regions of the outer surface of the tibia are smooth, although much of the surface of the shaft has been eroded. The entire shaft is markedly bowed laterally (Fig. 19), as in most basal mesoeucrocodylians (e.g., *A. tsangatsangana*, *Mahajangasuchus*, baurusuchids, *Notosuchus*) but contrasting with the straight shaft of basal crocodyliforms (e.g., *Orthosuchus*) and extant crocodylians. The distal end of the shaft is slightly bowed posteriorly, a feature present in *Iberosuchus* but absent in other crocodyliforms.

The distal expansion of the tibia is oriented obliquely to the transverse plane, differing from the more anteroposteriorly oriented distal expansion present in neosuchian crocodylians. The medial region of the distal surface of the tibia extends distally relative to the lateral region (Fig. 19E), a feature that distinguishes the tibia of basal mesoeucrocodylians (e.g., *A. tsangatsangana*, *Mahajangasuchus*, *Stratiotosuchus*, *Notosuchus* [MUC-PV 900]) from those of extant crocodylians.

The distal articular surface for the astragalus is 'L'-shaped in distal view, and divided into distinct lateral and medial facets (Fig. 19B). The lateral facet is elongate, narrow, flat, transversely

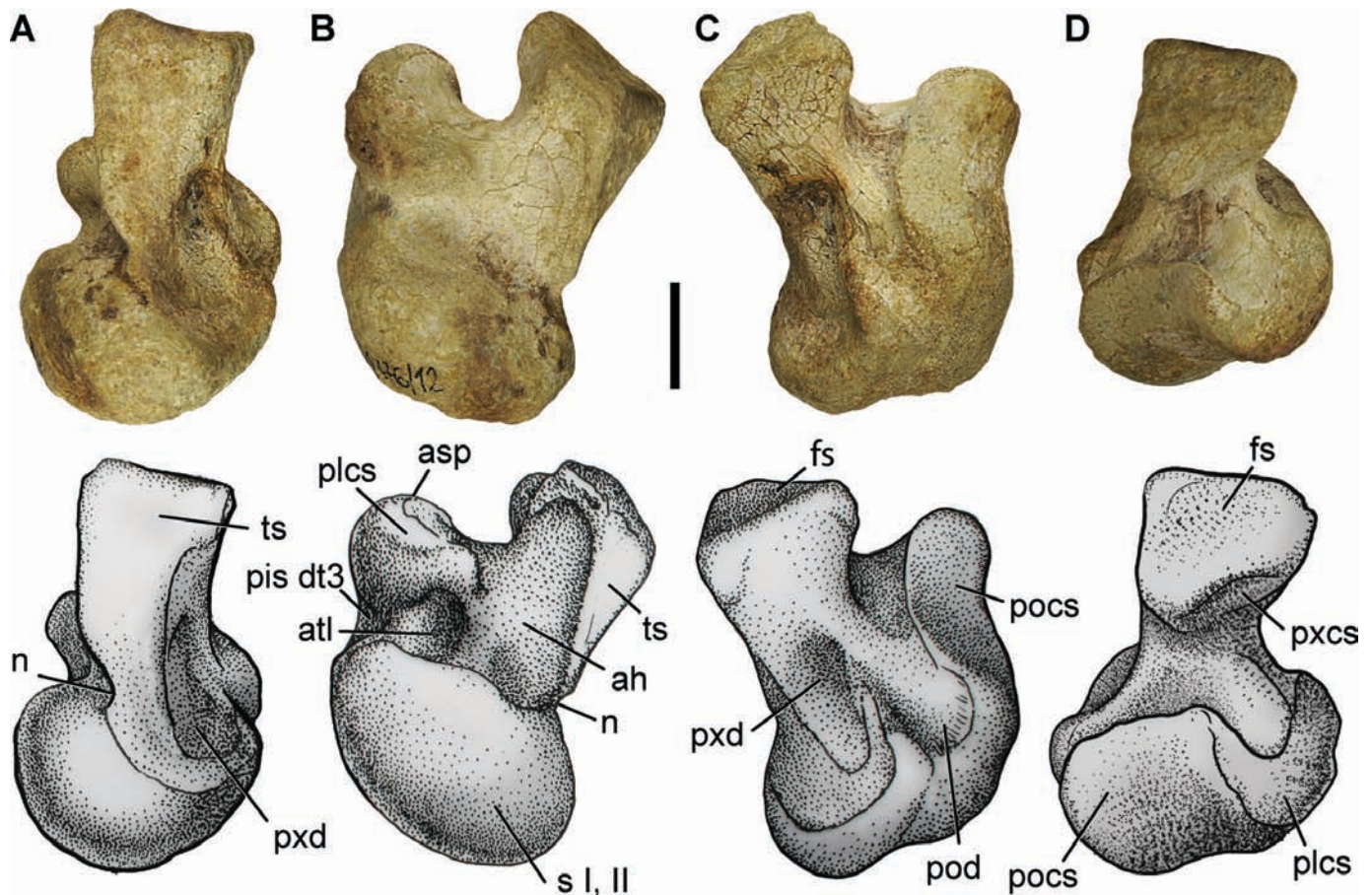


FIGURE 20. Right astragalus of *S. icaeorhinus* (MPEF-PV 1776), in **A**, proximal view, **B**, anterior view; **C**, posterior view; and **D**, lateral view. Scale bar equals 1 cm. (Color figure available online.)

oriented, and posteriorly inclined. The medial facet is broad, anteroposteriorly oriented, strongly convex, and distally projecting (Fig. 19B, E). The posterior surface of the distal tibia is marked by a well-developed oblique groove that extends proximally and laterally from the midpoint of the distal expansion of the tibia (Fig. 19A, B, E).

Astragalus—Four astragali are preserved among the available material of *S. icaeorhinus*. Proximally, the astragalus is divided into two articular facets for the distal facets of the tibia (Fig. 20A). The lateral tibial facet is flat, subrectangular, and tapers medially, bearing a well-developed notch at its anteromedial margin (also present in *Stratiotosuchus* and *Lomasuchus*, but not in other crocodyliforms). The medial tibial articular facet is reniform, slightly concave, and faces posteriorly.

The astragalus has a shallow proximal depression (Fig. 20A, C) located posterior and medial to the lateral facet for the tibia. *Simosuchus* and extant crocodylians have a much deeper depression proximal, where the posterior and internal tibial-astragalar ligaments attach (Brinkman, 1980). The largest astragali of *S. icaeorhinus* (MPEF-PV 3972) have a deeper proximal depression, although this is still much less developed than in extant crocodylians. Extant crocodylians also bear a vascular foramen within this depression (Riff, 2007), which is absent in *S. icaeorhinus* and other crocodyliforms.

The anterior surface of the astragalus has a large anterior astragalar hollow on its proximolateral corner, the planar calcaneal facet on its distolateral corner, and an extensive convex surface for the articulation of metatarsals I and II on its medial

region (Fig. 20B). The anterior astragalar hollow is a large and subtriangular, but relatively shallow, depression partially bounded proximally by the anterior margin of the lateral tibial facet, laterally by the anterior margin of the fibular facet, and medially by the large and rounded metatarsal facet. The anterior astragalar hollow is open laterally, because the planar and proximal calcaneal facets are not connected to each other in *S. icaeorhinus* (a condition also found in *Simosuchus* and baurusuchids). This morphology contrasts with the condition of most crocodyliforms (including *A. gomesii* and *Lomasuchus*), in which the planar and proximal calcaneal facets are connected to each other by an elevated ridge that bounds the lateral margin of the astragalar hollow. The distal apex of the astragalar hollow bears a rounded and distinct astragalar-tarsale ligament pit (Fig. 20B) that is proximally limited by a shallow ridge, a feature absent in crocodylians. Distal to this deep depression, the astragalus has a small surface for articulation with distal tarsal 3 proximally inset from the distal margin of the astragalus (Fig. 20B).

The fibular facet is located on the lateral surface of the dorsolateral process. The fibular facet is slightly concave and subtrapezoidal, with the proximodistal height of the anterior margin smaller than the posterior margin (Fig. 20D), as in *Lomasuchus*, *A. gomesii*, *Simosuchus*, and *Stratiotosuchus*. Other crocodyliforms have a subrectangular fibular facet.

The astragalus contacts the calcaneum on three distinct articular surfaces. The first, the proximal calcaneal facet ('dorsal astragalocalcaneal articular facet' sensu Sereno, 1991) is located

on the distal surface of the dorsolateral process of the astragalus (Fig. 20D). This facet faces distally and is slightly concave for its articulation with the medial half of the rounded dorsal calcaneal condyle. The second, the planar calcaneal facet ('ventral astragalocalcaneal articular facet' sensu Sereno, 1991) is a flat articular surface located on the laterodistal corner of the astragalus. This surface is crescentic and faces laterally (Fig. 20D), having at its posterior corner the astragalus peg. The planar calcaneal facet articulates with the longitudinally oriented planar astragalus facet of the calcaneum. The largest specimen of *S. icaeorhinus* (MPEF-PV 3972) bears a low ridge oriented proximodistally along the planar calcaneal facet, which is almost indistinguishable in the smaller specimens (MPEF-PV 1776). As noted above, the proximal and the planar calcaneal facets of *S. icaeorhinus* are completely separated from each other (Fig. 20D), creating a non-articular gap in the astragalocalcaneal articulation. The third, the posterior calcaneal facet or trochlea (Turner, 2006; Nascimento and Zaher, 2010), is located at the posterodistal corner of the astragalus. This surface is saddle-shaped, mediolaterally broad, and mediolaterally concave in posterior view (Fig. 20C, D). The astragalus trochlea extends laterally to the astragalus peg. The posterior calcaneal facet contacts the posterior (mediolaterally oriented) surface of the calcaneal socket. In posterior view, the astragalus trochlea is separated from the rounded articular surface for metatarsals I and II by a shallow notch. This

notch is located just distal to the proximal astragalus depression and encloses a shallow posterior depression (Fig. 20C). In extant crocodylians, the notch and associated depression are present and much more strongly developed, even in young specimens.

Calcaneum—Four calcanea are preserved. The calcaneal condyle occupies the anterior half of the calcaneum and is mediolaterally narrow in comparison with the posterior region (Fig. 21). The condyle is dorsoventrally deep and its flat lateral surface is approximately as deep as the calcaneal tuber (Fig. 21A). The proximal and anterior surface of the condyle is hemicylindrical, its medial half forms the proximal astragalus facet and its lateral half contacts the fibula. The plantar surface of the calcaneal condyle is flat and subrectangular (Fig. 21D), for contact with the proximal surface of distal tarsal 4. This facet in crocodylians has an oblique posterolateral margin, contrasting with the right-angled posterolateral corner of the rectangular facet of *S. icaeorhinus* and other basal mesoeucrocodylians (*A. tsangatsangana*, *Simosuchus*, *B. ableroi*).

The medial surface of the calcaneal condyle bears a deep calcaneal socket for the articulation with the astragalus peg. The socket is deepest at its posteroproximal corner, where the medial margin of the calcaneal condyle forms a shelf that overhangs the socket. The calcaneal socket is shallow along its anterior and plantar region, forming a planar astragalus facet (Fig. 21B) that contacts the planar calcaneal facet of the astragalus. The entire

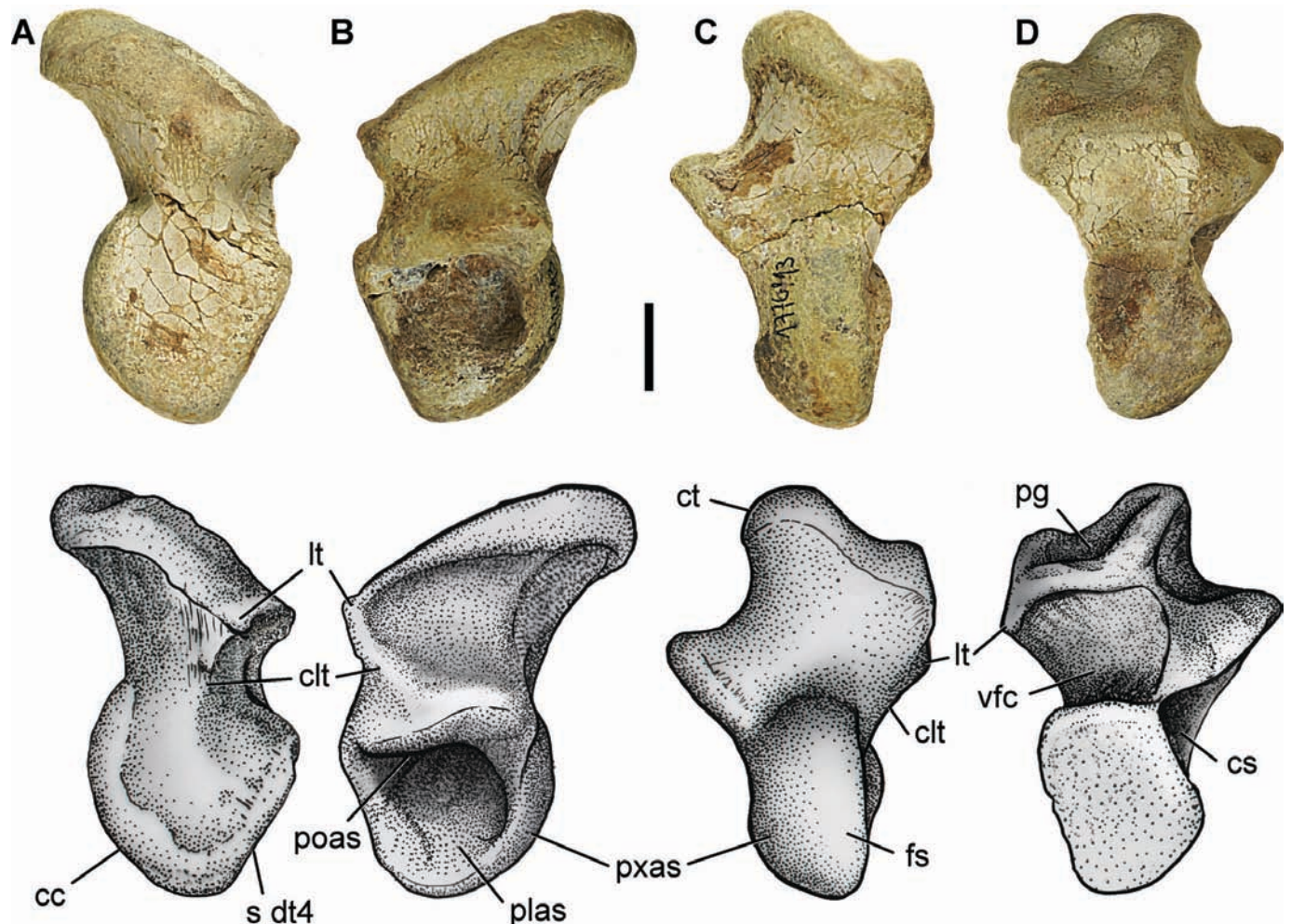


FIGURE 21. Left calcaneum of *S. icaeorhinus* (MPEF-PV 1776), in **A**, lateral view; **B**, medial view; **C**, proximal view; and **D**, distal view. Scale bar equals 1 cm. (Color figure available online.)

ventral margin of the socket is formed by a well-developed thick ridge. The anterior margin of the socket lacks the ridge that limits this socket in other crocodyliiforms. The posterior wall of the calcaneal socket is referred to as the posterior astragalar facet, projecting posteromedially from the posterior edge of the socket (Fig. 21C, D). The posterior astragalar facet forms an obtuse angle with the longitudinal axis of the calcaneal condyle of approximately 140 degrees. This facet is saddle-shaped and slightly convex mediolaterally, matching the shape of the posterior calcaneal surface of the astragalus. In anterior view, the posterior astragalar facet of the calcaneum is subtriangular, with proximal and lateral margins forming a right angle and an oblique medioplantar edge. Crocodylians have subparallel proximal and plantar edges and a broad and rounded medial edge. The lateral end of the proximal margin of the posterior astragalar facet curves gradually to meet the medial edge of the calcaneal condyle and form the shelf that overhangs the deepest region of the calcaneal socket (Fig. 21B–D).

The calcaneum bears a prominent posterolaterally directed tuber (Fig. 21C) that forms an angle of approximately 75 degrees relative to the transverse axis of the ankle joint (i.e., the axis of rotation). The degree of lateral deflection of the calcaneal tuber has been interpreted as functionally important (Parrish, 1986), but crocodyliiforms seem to possess continuous variation in the direction of the calcaneal tuber. In lateral view, the distal facet of the calcaneal condyle is orthogonal to the posterior margin of the tuber (Fig. 21A, B). The calcaneal tuber flares posteriorly and bears a vertical groove on its posterior surface for the *M. gastrocnemius* (Dilkes, 1999), the central region of which is broader and deeper than the dorsal and plantar ends. The tuber bears a well-developed lateral tubercle (Fig. 21). A fine horizontal ridge projects anteriorly to the lateral tubercle along the lateral surface of the calcaneum up to the condylar region. The lateral tubercle and associated ridge is more strongly developed in larger specimens (e.g., MPEF-PV 3972). Dorsally, the lateral surface of the tuber curves smoothly up to the horizontal dorsal surface of the tuber. All other crocodyliiforms have a well-developed dorsolateral ridge that extends along the tuber, separating its lateral and dorsal surfaces. The dorsal surface of the tuber is nearly flat and lacks the distinct dorsal fossa present just posteriorly to the calcaneal condyle in other crocodyliiforms (that is laterally bounded by the dorsolateral ridge).

The plantar surface of the tuber has a deep ventral fossa bounded medially by a ridge that connects the ventromedial angle of the tuber with the posteromedial corner of the plantar margin of the posterior astragalar surface of the calcaneum.

Distal Tarsal 4—Only distal tarsals 3 and 4 are ossified in extant crocodylians (Müller and Alberch, 1990). Specimen MPEF-PV 1776 preserves only distal tarsal 4. The anterior half of the proximal surface bears a flat, wide facet for contact with the ventral surface of the calcaneal condyle. Posteriorly, the proximal surface of distal tarsal 4 tapers abruptly to a narrow process (Fig. 22A), which projects proximally at its posterior end (Fig. 22C). In extant crocodylians (e.g., *Caiman*), this posterior tapering of distal tarsal 4 is much more gradual than in *S. icaeorhinus*. The posterior region of distal tarsal 4 is taller than the anterior region, expanding both proximally and distally (Fig. 22C). The distal deflection of the posterior end of distal tarsal 4 is, however, less developed than the proximal projection. This distal deflection of the posterior region rises smoothly in *S. icaeorhinus*, contrasting with the condition of *Caiman* in which the distal deflection is abrupt, creating a central notch in lateral view.

The lateral surface of distal tarsal 4 is flat for articulation with metatarsal V. This surface is subtriangular in lateral view and tapers anteriorly. Its dorsoventrally low anterior region faces distally and laterally whereas the deeper posterior region faces laterally (Fig. 22D). This contrasts with the condition of this sur-

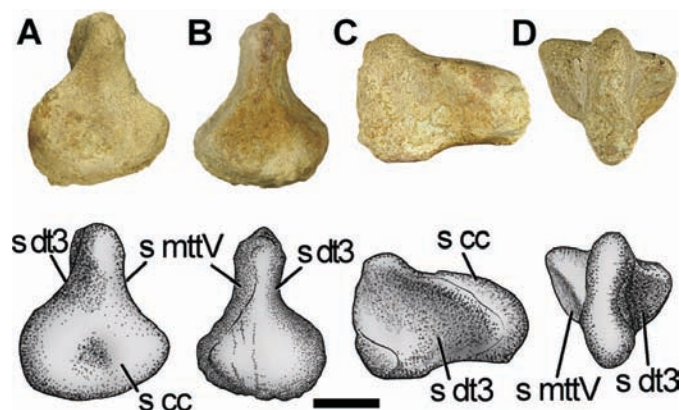


FIGURE 22. Left distal tarsal 4 of *S. icaeorhinus* (MPEF-PV 1776), in **A**, proximal view; **B**, distal view; **C**, medial view; and **D**, posterior view. Scale bar equals 1 cm. (Color figure available online.)

face in *Caiman*, where the anterior flat surface is proximodistally shorter. The lateral surface of distal tarsal 4 in *S. icaeorhinus* lacks the large fossa and associated foramen present on the posterior proximal corner of this surface in extant crocodylians.

The medial surface is concave for contact with distal tarsal 3, the posterior distal and anterior proximal corners each projecting medially (Fig. 22C, D). This surface is more concave than the lateral surface of distal tarsal 4 and lacks the medial foramen located on the distal region of the medial surface of crocodylians (e.g., *Caiman*).

The distal surface is similar in general outline to the proximal surface, although it is much smaller such that the lateral and medial margins of the proximal surface are visible in distal view (Fig. 22B). The broad anterior region is flat, contrasting with the mediolaterally bifaceted anterior surface of *Caiman*. The flat anterior margin of the distal face likely contacted the metatarsals III and IV, although these elements have not been preserved.

BODY PROPORTIONS AND SIZE ESTIMATES FOR *S. ICAEORHINUS*

The relatively complete postcranial skeleton of MPEF-PV 1776 provides insights into the overall size and body plan of *S. icaeorhinus*. Farlow et al. (2005) postulated several femoral measurements that may provide rough estimates of total body length and mass in crocodylians and some fossil mesoeucrocodylians. Applying the regression equations of Farlow et al. (2005) to femoral measurements of MPEF-PV 1776 results in estimates of total body length that vary from 2.2 to 3.1 m and a body mass of 52.2–113.5 kg (see Supplementary Data). These disparate results contrast with the much more accurate predictive value these regressions have for crocodylians. The femur of *S. icaeorhinus* is significantly more slender and elongate than the femora of extant crocodylians. As noted by Farlow et al. (2005) for other taxa (e.g., *Pristichampsus*, *Protosuchus*), regression equations that fit data for extant crocodylians are not necessarily good predictors for all crocodyliiforms. Here, we compare two of the measurements provided by Farlow et al. (2005), shoulder-hip length and femoral length, in *Alligator mississippiensis* and *S. icaeorhinus* to demonstrate the difference in body proportions between the latter and extant crocodylians. We used shoulder-hip length, rather than total body length, because the latter cannot be measured in MPEF-PV 1776.

Shoulder-hip length and femoral length are linearly correlated in different specimens of *A. mississippiensis* (Farlow et al., 2005) and can be expressed as a simple linear function (Fig. 23). The

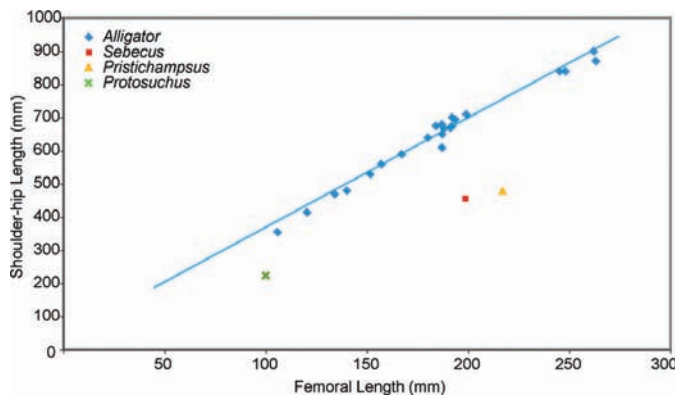


FIGURE 23. Scatter plot of shoulder-hip length versus femoral length for *A. mississippiensis*, *Pristichampsus* (data from Farlow et al., 2005), *Sebecus*, and *Protosuchus*. (Color figure available online.)

complete femur and the almost complete dorsal series of MPEF-PV 1776, however, differ from *A. mississippiensis*. The length of the dorsal series of this specimen can be estimated at 45.6 cm (see Supplementary Data), which is 2.3 times the length of the femur. This represents a proportionately more elongate femur for *S. icaeorhinus* with respect to body length, as evidenced by the shoulder-hip length versus femoral length plot (Fig. 23). Farlow et al. (2005) also noted that the eusuchian *Pristichampsus* (and other basal crocodylomorphs) had proportionately long limbs in comparison with extant crocodylians. Although *Pristichampsus* has an apparently more robust femur due to its remarkably well-developed areas of muscular insertions (C. Brochu, pers. comm.), it shares with *S. icaeorhinus* apparent similarities in their body-limb proportions (Fig. 23). Given that *S. icaeorhinus* and *Pristichampsus* are not phylogenetically related, their body-limb proportions may reflect similarities in their ecology including more terrestrial locomotion (Rauhe, 1995; Rossmann, 2000). The presence of proportionately long limbs may also be common among other terrestrial non-neosuchian crocodylians (e.g., *Protosuchus*; Fig. 23), possibly representing the plesiomorphic condition among crocodylomorphs.

PHYLOGENETIC RELATIONSHIPS

This new information on the postcranial anatomy of *S. icaeorhinus* was incorporated into a phylogenetic data set in order to analyze the phylogenetic relationships of this taxon. The data set is an extension of Pol and Powell (2011), which was in turn based on Pol et al. (2009). The character sampling was increased by adding 52 new postcranial characters and one character from Buckley and Brochu (1999) (see Supplementary Data). The data matrix is based on 347 characters scored in 88 taxa and was analyzed using equally weighted parsimony in TNT (Goloboff et al., 2008a, 2008b; see Supplementary Data). The analysis resulted in 432 most parsimonious trees (MPTs) of 1288 steps (consistency index [CI] = 0.328, retention index [RI] = 0.716).

The results of this phylogenetic analysis are identical to those of Pol and Powell (2011) regarding the internal topology of Sebecidae as well as the phylogenetic position of this clade, but have important differences in the relationships of Uruguaysuchidae (i.e., *Araripesuchus* + *Uruguaysuchus*) and peirosaurids (see below). All MPTs depict *S. icaeorhinus* nested within Sebecidae (Fig. 24), forming a clade with the two other species of *Sebecus* (*S. huilensis* and *S. querejazus*) and an undescribed taxon from the Lumbra Formation of northwestern Argentina (see Supplementary Data). Two taxa from the Eocene of Europe (*Ibero-*

suchus and *Bergisuchus*) are depicted as the closest relatives of Sebecidae in agreement with previous studies (Ortega et al., 1996, 2000; Company et al., 2005; Pol and Powell, 2011). This large clade of sebecids and allies is clustered with baurusuchids (i.e., *Baurusuchus*, *Cynodontosuchus*, *Stratiosuchus*, *Pabwehshi*), forming a monophyletic Sebecosuchia (sensu Gasparini, 1972) that is deeply nested within Notosuchia. The synapomorphic features of Sebecosuchia and Sebecidae are mainly based on craniomandibular and dental data (see Pol and Powell, 2011, and Supplementary Data for a complete list of synapomorphies) and alternative placements of Sebecidae as closer to peirosaurids (as proposed by Larsson and Sues, 2007) are moderately suboptimal (see below).

The addition of the 52 new postcranial characters enlarges the character sampling on the postcranium, reaching 27% of the character data in this study. The new information provided by these postcranial characters is discussed here from a phylogenetic perspective aiming to assess their relevance for solving the relationships of basal mesoeucrocodylians and the disputed affinities of Sebecidae.

Postcranial Evidence for Notosuchian Monophyly

The major difference in the topology of the MPTs of this study and that of Pol and Powell (2011) is the position of peirosaurids (and related forms) within Notosuchia. Peirosauridae has been depicted as more closely related to neosuchian crocodylians than to Notosuchia in most phylogenetic studies (Buckley and Brochu, 1999; Buckley et al., 2000; Ortega et al., 2000; Pol et al., 2004; Pol and Apesteguía, 2005; Turner and Calvo, 2005; Turner, 2006; Larsson and Sues, 2007; Turner and Buckley, 2008; Pol et al., 2009; Sereno and Larsson, 2009). In these studies, *Araripesuchus* was alternatively retrieved as closer to notosuchians than to Peirosauridae + Neosuchia or as closer to Peirosauridae + Neosuchia than to notosuchians.

The phylogenetic results obtained here provide a different arrangement of these clades, positioning Uruguaysuchidae as the sister group of Peirosauridae, but placing this clade as part of Notosuchia rather than closer to Neosuchia (Fig. 24). Therefore, all peirosaurids, uruguaysuchids, and ziphosuchians (including Baurusuchidae and the derived Sebecidae) are retrieved in a large clade that includes all basal mesoeucrocodylians recorded in the Cretaceous of Gondwana. The monophyly of this group is not novel to this analysis and several characters have been proposed in phylogenetic analyses during the last decade that suggested the close affinities of all these forms (see below). In fact, based on a phylogenetic analysis of these taxa, Carvalho et al. (2004) coined the term Gondwanasuchia for a group with similar taxonomic content. Similarly, Turner and Sertich (2010) also retrieved a large monophyletic clade similar in taxonomic composition, using a data set that was also based on an expansion of Pol et al. (2009). The internal relationships at the base of this clade are, however, different from those obtained in this study. Turner and Sertich (2010) referred to this clade as Notosuchia, but expressed concerns regarding the lack of coherence with the historical taxonomic content of Notosuchia (Gasparini, 1971; namely the inclusion of peirosaurids within this clade). We agree with such concerns, but have followed their use of Notosuchia (Fig. 24) for this large clade, which also fits the phylogenetic definition of Notosuchia given by Sereno et al. (2001). In our phylogenetic analysis, Notosuchia includes a large clade that includes *Libycosuchus*, *Notosuchus*, and sebecosuchians, which we refer to as Ziphosuchia (Fig. 24), because it matches the taxonomic content of Ziphosuchia (sensu Ortega et al., 2000) and the node-based phylogenetic definition of this clade given by Carvalho et al. (2004). A similar decision on the use of Ziphosuchia was adopted by Turner and Sertich (2010).

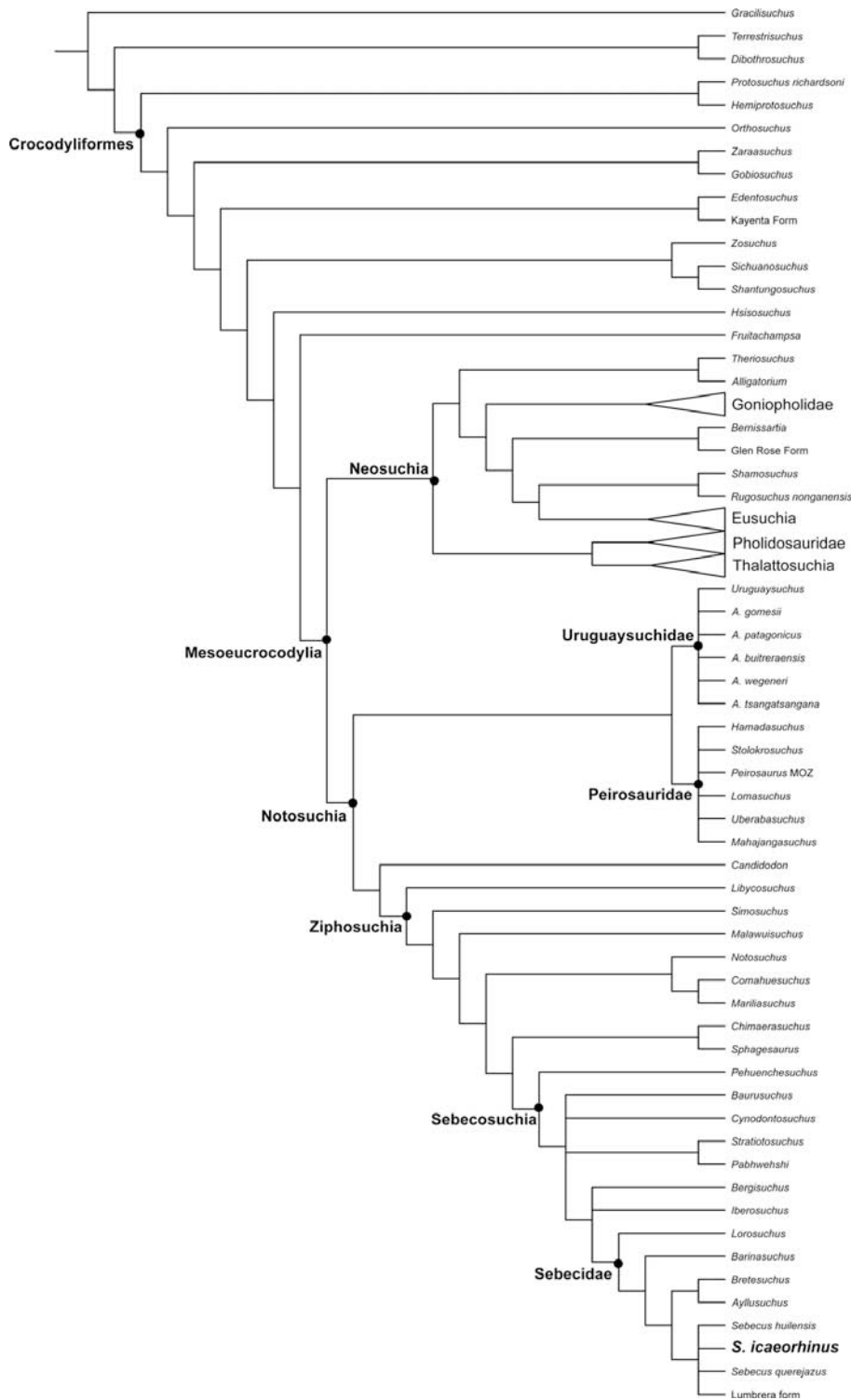


FIGURE 24. Strict consensus of the 432 MPTs obtained in the phylogenetic analysis. Some neosuchians clades have been collapsed in this tree (see Supplementary Data for further details).

In this analysis, Notosuchia is diagnosed by 23 unambiguous synapomorphies present in all MPTs, including both cranial and postcranial features (see Supplementary Data). As mentioned above, part of this phylogenetic signal was already present in the craniomandibular characters of the original data set (e.g., characters 23, 29, 69, 70, 71, 171, 186, 284) and had been added to by successive studies (Clark, 1994; Ortega et al., 2000; Pol and Apesteguía, 2005; Larsson and Sues, 2007; see Turner and

Sertich, 2010, for a discussion of some cranial synapomorphies). As these characters were present in most recently published studies, the craniomandibular signal was already present but was comparatively weak, so that topologies depicting the inclusion of peirosaurids within Notosuchia were slightly suboptimal (e.g., Pol and Powell, 2011) or poorly supported (e.g., Turner and Sertich, 2010). However, 15 of the 23 unambiguous synapomorphic features of Notosuchia retrieved in this study are from

the postcranial skeleton of these forms. Some characters were already identified and include the rod-like morphology of at least some cervical vertebra (character 90.1; modified from Clark, 1994), anteriorly projected axial prezygapophysis (character 152.1; Pol, 2003), sigmoidal anterior margin of femur (character 157.1; Buckley and Brochu, 1999), posteriorly deflected proximal region of fibula (character 272.1; Turner, 2006), and expanded scapular blade (character 305.1; Buckley and Brochu, 1999).

The new postcranial characters of this data set provide decisive support for the monophyly of the large clade that clusters peirosaurids within Notosuchia, including nine postcranial synapomorphies. These include derived features of the axial skeleton, such as the dorsally projected and strongly curved prezygapophysis of the anterior cervicals (character 296.1), dorsal vertebrae 4 to 9 showing a gradual dorsal migration of the parapophyses (character 299.1), distinct rounded depression on the lateral surface of the neural arch between the spine and the postzygapophysis of middle to posterior dorsals (character 302.1), transverse process and articular facet of postzygapophysis dorsoventrally leveled in middle dorsals (character 303.1). New synapomorphic features of the appendicular skeleton include the presence of a deep circular depression on the posterior surface of the proximal humerus for the insertion of the M. scapulohumeralis caudalis (character 314.1), subrectangular posterior end of the postacetabular process of the ilium (character 326.1), ventral margin of the postacetabular iliac process horizontally directed (character 327.1) and located well below the level of the acetabular roof (character 328.1), and the trapezoidal shape of the fibular facet on the astragalus (character 343.2).

Notosuchia has relatively low support values (Bremer support = 2, bootstrap = 28%, jackknife = 35%; see Supplementary Data) despite the large number of postcranial features shared by notosuchians mentioned above. The low support values, however, are caused by the problematic affinities of two taxa that bear a conflicting combination of characters (*Lorosuchus* and *Stolokrosuchus*) and two highly incomplete taxa (*Pehuenchesuchus* and *Cynodontosuchus*). If the alternative positions of these four taxa are ignored during the support analysis, the resulting values are higher (Bremer support = 4, bootstrap = 63%, jackknife = 74%; see Supplementary Data). Furthermore, in order to test the strength of the current position of peirosaurids in comparison with the more traditional placement of peirosaurids as closer to Neosuchia, heuristic tree searches were conducted constraining these forms to be closer to neosuchians. The resulting topologies are 10 steps longer than the MPTs of the unconstrained search. The new postcranial characters used in this analysis are decisive in supporting the inclusion of peirosaurids within Notosuchia.

Postcranial Evidence for Sebecosuchian Monophyly

As noted above, a long-standing debate exists regarding the evolutionary origins of Sebecidae, which is intimately related to testing sebecosuchian monophyly (Sebecidae + Baurusuchidae) versus alternative placements for sebecids as closer to peirosaurids (Sebecia sensu Larsson and Sues, 2007). The evidence supporting these alternative placements of Sebecidae was, until now, based on craniomandibular characters. For instance, all recognized synapomorphic features of Sebecosuchia in previous phylogenetic studies were exclusively focused on the derived condition of the teeth and mandible of sebecids and baurusuchids (e.g., Ortega et al., 2000; Pol and Powell, 2011). Many of these characters had been interpreted as adaptations to carnivory (e.g., mandibular, caniniform, compressed teeth with serrated margins) and discussed in earlier studies of these forms (e.g., Colbert, 1946; Gasparini, 1972; Buffetaut, 1980). Similarly, the proposed synapomorphies of Sebecia (Larsson and Sues, 2007) were centered on derived features of the palate shared by sebecids

and peirosaurids. The exclusive reliance on craniomandibular characters was caused by the lack of knowledge on the postcranial anatomy of sebecids (unknown until this contribution) and the two possibly related groups. Peirosaurid postcranial anatomy is poorly known, but the well-preserved *Mahajangasuchus* provided a source of comparison since its publication (Buckley and Brochu, 1999), whereas there was a complete absence of detailed descriptions of baurusuchid postcrania until recently (Nascimento and Zaher, 2010; Riff and Kellner, 2011).

The incorporation of new postcranial characters and completion of character scorings provided by recent contributions on the postcranium of basal mesoeucrocodylians (*A. tsangatsangana*, *Simosuchus*, *Notosuchus*, *Baurusuchus*, *Stratiotosuchus*) resulted in numerous derived postcranial characters that diagnose different nodes within Notosuchia in this phylogenetic study. These postcranial characters provide additional support for the deeply nested position of *Sebecus* (and Sebecidae) within this clade, as part of Sebecosuchia (Fig. 24).

This set of characters includes two previously proposed characters that can now be scored in several notosuchids, baurusuchids, and *Sebecus*: rod-like neural spines in all cervicals (character 90.2 [modified from Clark, 1994]; present in *Simosuchus* and more-derived notosuchians) and an extensive and laterally projected supracetabular crest (character 116.2 [modified from Buscalioni and Sanz, 1988]; present in *Notosuchus* and more-derived notosuchians).

The appendicular skeleton of ziphosuchian crocodyliforms (including baurusuchids and *Sebecus*) is highly modified in comparison with the condition of other crocodyliforms. This is represented by six of the new appendicular characters that represent the successive transformation of the appendicular skeleton along the evolution of Ziphosuchia, all of which are absent in peirosaurids but have the derived condition in *Sebecus*.

Simosuchus and more-derived notosuchians (including *Sebecus*) share the presence of two derived characters: a proximodistally elongated articular surface for the ulna on the radiale (character 319.1), and planar and proximal articular surfaces on the astragalus for the calcaneum separated to form two distinct facets (character 339.1). *Notosuchus* and more-derived forms (including *Sebecus*) share the presence of two further apomorphic characters: medially displaced proximal one-third of the deltopectoral crest (character 311.1), and articular surface for the ulna on the radiale facing posteriorly (character 318.1). Finally, the postcranium of baurusuchids and *Sebecus* also shares two derived postcranial features that are absent in other ziphosuchians or notosuchians: vertical orientation of the insertion area of the M. subscapularis above the internal tuberosity of the humerus (character 309.1), and distal end of the deltopectoral crest extending medially beyond the lateromedial midpoint of the humeral shaft (character 312.1).

Many of the nodes within Ziphosuchia (including Sebecosuchia) have low values of nodal support (Bremer values are 1 or 2, bootstrap/jackknife frequencies below 50%; see Supplementary Data). As discussed by Pol and Powell (2011), this is mostly due to the highly unstable behavior of some fragmentary taxa in suboptimal trees (e.g., *Pehuenchesuchus*, *Cynodontosuchus*). Ignoring the alternative positions of these taxa in suboptimal trees increases the support of some nodes (e.g., *Notosuchus* and more-derived forms, including Sebecidae; see Supplementary Data). Furthermore, the degree of support for sebecosuchian monophyly versus the alternative placement proposed for sebecids (i.e., monophyly of Sebecia sensu Larsson and Sues, 2007) can be tested through the use of constrained searches. When a heuristic tree search is conducted forcing Sebecidae to be outside Ziphosuchia (i.e., constraining the non-monophyly of Sebecosuchia), the resulting phylogenetic trees depict Sebecidae (and *Iberosuchus* + *Bergisuchus*) as the sister group of Peirosauridae. These trees are five steps longer than the MPTs of the

unconstrained search. The addition of the new postcranial characters notably increases the support for sebecosuchian monophyly, given that when the 52 new characters are eliminated from the matrix, the difference between the unconstrained search (sebecosuchian topology) and the constrained search (sebecian topology) is reduced to only one step.

The affinities of *Iberosuchus* with Sebecidae have been supported by most previous phylogenetic studies, but are reinforced in this study with the identification of four new postcranial synapomorphies: concave and proximally facing shelf that separates the anterior surface of humerus from the distal articular surface (character 316.1), proximodistally short greater trochanter lacking a well-developed lateral ridge (character 331.1; paralleled in *Mahajangasuchus*), medial edge of the greater trochanter prominent forming a sharp crest offset from the medial surface of the femur (character 332.1), and distal half of tibial shaft posteriorly bowed in lateral view (character 335.1).

CONCLUSIONS

The postcranial anatomy of *S. icaeorhinus* reveals the presence of multiple autapomorphic features of this taxon, mirroring the highly modified skull morphology that has drawn attention to this taxon since its discovery (Simpson, 1937; Colbert, 1946; Gasparini, 1972). Because this is the first sebecid for which a postcranium is known, some of these features may, in fact, represent potential synapomorphies of different nodes of Sebecidae.

The proportions of the femur relative to the vertebral column indicate that *S. icaeorhinus* was a long-limbed crocodyliform in comparison with neosuchian crocodyliforms, resembling the proportions of the high-snouted and ziphodont eusuchian *Pristichampsus* and other basal crocodyliforms (e.g., *Protosuchus*).

The comparative study of the postcranium of *Sebecus* revealed new phylogenetically relevant information that resulted in the discovery of numerous characters that support the inclusion of peirosaurids within Notosuchia, a clade with important implications for understanding the evolutionary and biogeographic history of Cretaceous crocodyliforms from the southern hemisphere. Although some members of this clade can be positioned outside Notosuchia with few extra steps (e.g., *Stolokrosuchus*, *Lorosuchus*), alternative topologies that place peirosaurids closer to neosuchians are markedly suboptimal.

The new postcranial characters also increase the support for the monophyly of Sebecosuchia as a clade deeply nested within Notosuchia, increasing the tree length difference for alternative positions of Sebecidae (as closer to peirosaurids). In this way, Sebecidae (and related forms from the Eocene of Europe) are interpreted as the only lineage of the ecologically and taxonomically diverse notosuchians that survived the Cretaceous–Paleogene mass extinction.

The derived postcranial similarities between *Sebecus*, baurusuchids, and the small-bodied notosuchians (e.g., *Notosuchus*) are not only phylogenetically relevant, but also shed light on some functional aspects of this clade. Most of these similarities are centered on modifications of the appendicular skeleton, such as changes in the insertion of glenohumeral musculature, lateral extension of the supracetabular crest, and changes in the astragalo-calcaneal articular facets. Despite these similarities, small-bodied notosuchians and sebecosuchians have remarkable differences in their skull and dental anatomy, as well as in their inferred dietary habits. **Thus, this ecologically diverse and successful clade of Cretaceous–Cenozoic mesoeucrocodylians seems to have shared a basic set of postcranial features probably related to terrestriality.**

ACKNOWLEDGMENTS

The specimens described were found during fieldwork led by A. López-Arbarello (MPEF-PV 1776) and by M. de la Fuente

(PIP-CONICET 00795). Research for this contribution was possible due to the grant PICT 0736 (Agencia Nacional de Promoción de Ciencia y Técnica). This is JML's R-50 contribution to the Instituto de Estudios Andinos Don Pablo Groeber. J. González completed the drawings. We thank Aluar Aluminio Argentino and Mr. J. Groizard for access to the SEM lab. We thank F. Ortega for comments on the manuscript and access to specimens of *Iberosuchus*. We also thank the participants of the field expeditions: P. Puerta, M. Cardenas, J. Sterli, I. Maniel, B. von Baczko, M. Ramírez, and D. Castro. The specimens were prepared by L. Reiner. TNT is a free program made available by the Willi Hennig Society.

LITERATURE CITED

- Andreis, R. R. 1977. Geología del área de Cañadón Hondo, Depto Escalante, provincia del Chubut, República Argentina. *Obra Centenario de La Plata* 4:77–102.
- Brinkman, D. 1980. The hind limb step cycle of *Caiman sclerops* and the mechanics of the crocodile tarsus and metatarsus. *Canadian Journal of Zoology* 46:1–23.
- Buckley, G. A., and C. A. Brochu. 1999. An enigmatic new crocodile from the Upper Cretaceous of Madagascar. *Special Papers in Palaeontology* 60:149–175.
- Buckley, G. A., C. A. Brochu, D. W. Krause, and D. Pol. 2000. A pug-nosed crocodyliform from the Late Cretaceous of Madagascar. *Nature* 405:941–944.
- Buffetaut, E. 1980. Histoire biogéographique des Sebecosuchia (Crocodylia, Mesosuchia): un essai d'interprétation. *Annales de Paléontologie (Vertébrés)* 66:1–18.
- Buffetaut, E. 1991. *Itasuchus* Price, 1955; pp. 348–350 in J. G. Maisey (ed.), *Santana Fossils: An Illustrated Atlas*. TFH Publications Inc., Neptune, New Jersey.
- Buffetaut, E., and L. Marshall. 1991. A new crocodylian, *Sebecus querejazus*, nov. sp. (Mesosuchia, Sebecidae) from the Santa Lucía Formation (Early Paleocene) at Vila Vila, Southcentral Bolivia; pp. 545–557 in R. Suárez-Soruco (ed.), *Fósiles y Facies de Bolivia. Volume I, Vertebrados*. Revista Técnica de YPF, Santa Cruz, Bolivia.
- Busbey, A. B. I. 1986. New material of *Sebecus* cf. *huilensis* (Crocodylia: Sebecosuchidae) from the Miocene of La Venta Formation of Colombia. *Journal of Vertebrate Paleontology* 6:20–27.
- Buscalioni, A. D., and J. L. Sanz. 1988. Phylogenetic Relationships of the Atoposauridae (Archosauria, Crocodylomorpha). *Historical Biology* 1:233–250.
- Carrano, M. T., and J. R. Hutchinson. 2002. Pelvis and hindlimb musculature of *Tyrannosaurus rex* (Dinosauria: Theropoda). *Journal of Morphology* 253:207–228.
- Carvalho, I. d. S., L. C. B. Ribeiro, and L. d. S. Avilla. 2004. *Uberabasuchus terrificus* sp. nov., a New Crocodylomorpha from the Bauru Basin (Upper Cretaceous), Brazil. *Gondwana Research* 7:975–1002.
- Clark, J. M. 1986. Phylogenetic relationships of the Crocodylomorph Archosaurs. Unpublished Ph.D. dissertation, University of Chicago, Chicago, Illinois, 556 pp.
- Clark, J. M. 1994. Patterns of evolution in Mesozoic Crocodyliformes; pp. 84–97 in N. C. Fraser and H.-D. Sues (eds.), *In the Shadow of the Dinosaurs. Early Mesozoic Tetrapods*, Cambridge University Press, Cambridge, U.K.
- Colbert, E. H. 1946. *Sebecus*, representative of a peculiar suborder of fossil Crocodylia from Patagonia. *Bulletin of the American Museum of Natural History* 87:217–270.
- Company, J., X. Pereda Suberbiola, J. I. Ruiz-Omeñaca, and A. D. Buscalioni. 2005. A new species of *Doratodon* (Crocodyliformes: Ziphosuchia) from the Late Cretaceous of Spain. *Journal of Vertebrate Paleontology* 25:343–353.
- Dilkes, D. W. 1999. Appendicular myology of the hadrosaurian dinosaur *Maiasaura peeblesorum* from the Late Cretaceous (Campanian) of Montana. *Transactions of the Royal Society of Edinburgh: Earth Sciences* 90:87–125.
- Farlow, J. O., G. R. Hurlburt, R. M. Elsey, A. R. C. Britton, and W. J. Langston. 2005. Femoral dimensions and body size of *Alligator mississippiensis*: estimating the size of extinct mesoeucrocodylians. *Journal of Vertebrate Paleontology* 25:354–369.
- Feruglio, E. (ed.) 1949. *Descripción Geológica de la Patagonia* 2. Imprenta Coni, Buenos Aires, 349 pp.

- Fiorelli, L. E. 2005. Nuevos Restos de *Notosuchus terrestris* Woodward, 1896 (Crocodyliformes: Mesoeucrocodylia) del Cretácico Superior (Santoniano) de la Provincia de Neuquén, Patagonia, Argentina. Licenciatura Thesis, Universidad Nacional de Córdoba, Córdoba, Argentina, 80 pp.
- Frey, E. 1988. Das Tragsystem der Krocodile—eine biomechanische und phylogenetische Analyse. Stuttgarter Beiträge zur Naturkunde (Serie A) 426:1–60.
- Gasparini, Z. 1971. Los Notosuchia del Cretácico de América del Sur como un nuevo Infraorden de los Mesosuchia (Crocodylia). *Ameghiniana* 8:83–103.
- Gasparini, Z. 1972. Los Sebecosuchia (Crocodylia) del Territorio Argentino. Consideraciones sobre su “status” taxonómico. *Ameghiniana* 9:23–34.
- Gasparini, Z. 1984. New Tertiary Sebecosuchia (Crocodylia: Mesosuchia) from Argentina. *Journal of Vertebrate Paleontology* 4:85–95.
- Gasparini, Z. B. 1996. Biogeographic evolution of the South American crocodylians. *Münchner Geowissenschaftliche Abhandlungen* 30:159–184.
- Gasparini, Z., M. Fernandez, and J. Powell. 1993. New Tertiary sebecosuchians (Crocodylomorpha) from South America: phylogenetic implications. *Historical Biology* 7:1–19.
- Gasparini, Z., D. Pol, and L. A. Spalletti. 2006. An unusual marine crocodyliform from the Jurassic–Cretaceous boundary of Patagonia. *Science* 311:70–73.
- Georgi, J. A., and D. W. Krause. 2010. Postcranial axial skeleton of *Simosuchus clarki* (Crocodyliformes: Notosuchia) from the Late Cretaceous of Madagascar. *Society of Vertebrate Paleontology Memoir* 10:99–121.
- Goloboff, P. A., J. S. Farris, and K. C. Nixon. 2008a. TNT, a free program for phylogenetic analysis. *Cladistics* 24:774–786.
- Goloboff, P. A., J. S. Farris, and K. C. Nixon. 2008b. TNT: Tree Analysis Using New Technologies. Program and documentation available from the authors and at <http://www.zmuc.dk/public/phylogeny>. Accessed May 2011.
- Gomani, E. M. 1997. A crocodyliform from the Early Cretaceous dinosaur beds, northern Malawi. *Journal of Vertebrate Paleontology* 17:280–294.
- Hay, O. P. 1930. Second Bibliography and Catalogue of the Fossil Vertebrata of North America 2. Carnegie Institute, Washington, D.C., 1074 pp.
- Hutchinson, J. R. 2001a. The evolution of femoral osteology and soft tissues on the line to extant birds (Neornithes). *Zoological Journal of the Linnean Society* 131:169–197.
- Hutchinson, J. R. 2001b. The evolution of pelvic osteology and soft tissues on the line to extant birds (Neornithes). *Zoological Journal of the Linnean Society* 131:123–168.
- Hutchinson, J. R. 2002. The evolution of hindlimb tendons and muscles on the line to crown-group birds. *Comparative Biochemistry and Physiology Part A* 133:1051–1086.
- Langston, W. J. 1965. Fossil crocodylians from Colombia and the Cenozoic history of the Crocodylia in South America. University of California Publications in Geological Sciences 52:1–98.
- Langston, W. J., and Z. B. Gasparini. 2007. Crocodylians, *Gryposuchus*, and the South American gavials; pp. 113–154 in R. Kay, R. Madden, R. Cifelli, and J. Flynn (eds.), *Vertebrate Paleontology in the Neotropics. The Miocene Fauna of La Venta, Colombia*. Smithsonian Institution Press, Washington, D.C.
- Larsson, H. C. E., and H.-D. Sues. 2007. Cranial osteology and phylogenetic relationships of *Hamadasuchus rebouli* (Crocodyliformes: Mesoeucrocodylia) from the Cretaceous of Morocco. *Zoological Journal of the Linnean Society* 149:533–567.
- Legasa, O., A. D. Buscalioni, and Z. Gasparini. 1994. The serrated teeth of *Sebecus* and the iberocretanian crocodile, a morphological and ultrastructural comparison. *Studia Geologica Salmanticensia* 29:127–144.
- Meers, M. B. 2003. Crocodylian forelimb musculature and its relevance to Archosauria. *The Anatomical Record Part A* 274A:891–916.
- Molnar, R. E. 2010. A new reconstruction of the skull of *Sebecus icaeorhinus* (Crocodyliformes: Sebecosuchia) from the Eocene of Argentina. *Brazilian Geographical Journal: Geosciences and Humanities Research Medium* 1:314–330.
- Müller, G. B., and P. Alberch. 1990. Ontogeny of the limb skeleton in *Alligator mississippiensis*: developmental invariance and change in the evolution of archosaur limbs. *Journal of Morphology* 203:151–164.
- Nascimento, P. M., and H. Zaher. 2010. A new species of *Baurusuchus* (Crocodyliformes, Mesoeucrocodylia) from the Upper Cretaceous of Brazil, with the first complete postcranial skeleton described for the family Baurusuchidae. *Papéis Avulsos de Zoologia* 50:323–361.
- Novas, F. E. 1993. New information on the systematics and postcranial skeleton of *Herreasaurus ischigualastensis* (Theropoda: Herreasauridae) from the Ischigualasto Formation (Upper Triassic) of Argentina. *Journal of Vertebrate Paleontology* 13:400–423.
- Ortega, F. 2004. Historia evolutiva de los cocodrilos Mesoeucrocodylia. Ph.D. dissertation, Universidad Autónoma de Madrid, Madrid, 350 pp.
- Ortega, F., A. D. Buscalioni, and Z. B. Gasparini. 1996. Reinterpretation and new denomination of *Atacisaurus crassiproratus* (middle Eocene; Issel, France) as cf. *Iberosuchus* (Crocodylomorpha: Metasuchia). *Geobios* 29:353–364.
- Ortega, F., Z. B. Gasparini, A. D. Buscalioni, and J. O. Calvo. 2000. A new species of *Araripesuchus* (Crocodylomorpha, Mesoeucrocodylia) from the Lower Cretaceous of Patagonia (Argentina). *Journal of Vertebrate Paleontology* 20:57–76.
- Paolillo, A., and O. J. Linares. 2007. Nuevos cocodrilos Sebecosuchia del Cenozoico Suramericano (Mesosuchia: Crocodylia). *Paleobiologia Neotropical* 3:1–25.
- Parrish, J. M. 1986. Locomotor adaptations in the hindlimb and pelvis of the Thecodontia. *Hunteria* 1:1–35.
- Paula-Couto, C. 1970. Evolução de comunidades, modificações faunísticas e integrações bióticas dos vertebrados cenozóicos do Brasil. *Congreso Latinoamericano de Zoología, Actas* 4:907–930.
- Piatnitzky, A. 1931. Observaciones estratigráficas sobre las tobas con mamíferos del Terciario inferior en el valle del río Chico (Chubut). *Boletín de Informaciones Petroleras* 85:617–634.
- Pol, D. 2003. New remains of *Sphagesaurus huenei* (Crocodylomorpha: Mesoeucrocodylia) from the Late Cretaceous of Brazil. *Journal of Vertebrate Paleontology* 23:817–831.
- Pol, D. 2005. Postcranial remains of *Notosuchus terrestris* Woodward (Archosauria: Crocodyliformes) from the Upper Cretaceous of Patagonia, Argentina. *Ameghiniana* 42:21–38.
- Pol, D., and S. Apesteguía. 2005. New *Araripesuchus* remains from the early Late Cretaceous (Cenomanian–Turonian) of Patagonia. *American Museum Novitates* 3490:1–38.
- Pol, D., and J. Powell. 2011. A new basal mesoeucrocodylian from the Rio Loro Formation (Paleocene) of northwestern Argentina. *Zoological Journal of the Linnean Society* 163:S7–S36.
- Pol, D., A. H. Turner, and M. A. Norell. 2009. Morphology of the Late Cretaceous crocodylomorph *Shamosuchus djadochtaensis* and a discussion of neosuchian phylogeny as related to the origin of Eusuchia. *Bulletin of American Museum of Natural History* 324:1–103.
- Pol, D., S.-A. Ji, J. M. Clark, and L. M. Chiappe. 2004. Basal crocodylians from the Lower Cretaceous Tugulu Group (Xinjiang, China), and the phylogenetic position of *Edentosuchus*. *Cretaceous Research* 25:603–622.
- Prasad, G. V. R., and F. d. Broin. 2002. Late Cretaceous crocodile remains from Naskal (India): comparisons and biogeographic affinities. *Anales de Paléontologie* 88:19–71.
- Raigemborn, M. S., J. M. Krause, E. S. Bellosi, and S. D. Matheos. 2010. Redefinición estratigráfica del Grupo Río Chico (Paleógeno inferior), en el norte de la cuenca del Golfo San Jorge, Chubut, Argentina. *Revista de la Asociación Geológica Argentina* 67:239–256.
- Rauhe, M. 1995. Die Lebensweise und Ökologie der Geiseltal-Krokodilier—Abschied von traditionellen Lehrmeinungen. *Hallesches Jahrbuch für Geowissenschaften* 17:65–80.
- Riff, D. 2007. Anatomia apendicular de *Stratiosuchus maxhechti* (Baurusuchidae, Cretáceo Superior do Brasil) e análise filogenética dos Mesoeucrocodylia. Ph.D. dissertation, Universidade Federal do Rio de Janeiro, Rio de Janeiro, 395 pp.
- Riff, D., and A. W. A. Kellner. 2001. On the dentition of *Baurusuchus pacheoi* Price (Crocodyliformes, Metasuchia) from the Upper Cretaceous of Brazil. *Boletim do Museu Nacional, Nova Série, Geologia* 59:1–15.
- Riff, D., and A. W. A. Kellner. 2011. Baurusuchids crocodylians as theropod mimics: clues from the appendicular morphology of *Stratiosuchus maxhechti* (Upper Cretaceous of Brazil). *Zoological Journal of the Linnean Society* 163:S37–S56.
- Romer, A. S. 1923. Crocodylian pelvic muscles and their avian and reptilian homologues. *Bulletin of the American Museum of Natural History* 48:533–551.

- Rossmann, T. 2000. Studien an känozoischen Krokodilen: 5. Biomechanische Untersuchung am poskranialen Skelett des paläogenen Krokodils *Pristichampsus rollinatus* (Eusuchia: Pristichampsidae). Neues Jahrbuch für Geologie und Paläontologie, Abhandlungen 217:289–330.
- Rusconi, C. 1933. Sobre reptiles Cretaceous del Uruguay (*Uruguaysuchus aznarezi*, n. g. n. sp) y sus relaciones con los notosúquidos de Patagonia. Boletín Instituto de Geología y Perforaciones Montevideo Uruguay 19:1–64.
- Schaeffer, B. 1947. An Eocene serranid from Patagonia. American Museum Novitates 1331:1–9.
- Sereno, P. C. 1991. Basal archosaurs: phylogenetic relationships and functional implications. Society of Vertebrate Paleontology Memoir 2:1–53.
- Sereno, P. C., and H. C. E. Larsson. 2009. Cretaceous crocodyliforms from the Sahara. ZooKeys 28:1–143.
- Sereno, P. C., H. C. E. Larsson, C. A. Sidor, and B. Gado. 2001. The giant crocodyliform *Sarcosuchus* from the Cretaceous of Africa. Science 294:1516–1519.
- Sereno, P. C., C. A. Sidor, H. C. E. Larsson, and B. Gado. 2003. A new notosuchian from the Early Cretaceous of Niger. Journal of Vertebrate Paleontology 23:477–482.
- Sertich, J. J. W., and J. R. Groenke. 2010. Appendicular Skeleton of *Simosuchus clarki* (Crocodyliformes: Notosuchia) from the Late Cretaceous of Madagascar. Society of Vertebrate Paleontology Memoir 10:122–153.
- Simpson, G. G. 1935. Occurrence and relationships of the Río Chico fauna of Patagonia. American Museum Novitates 818: 1–21.
- Simpson, G. G. 1937. New reptiles from the Eocene of South America. American Museum Novitates 927:1–3.
- Soto, M., D. Pol, and D. Perea. 2011. A new specimen of *Uruguaysuchus aznarezi* (Crocodyliformes: Notosuchia) from the Cretaceous of Uruguay and its phylogenetic relationships. Zoological Journal of the Linnean Society 163:S173–S198.
- Turner, A. H. 2006. Osteology and phylogeny of a new species of *Araripesuchus* (Crocodyliformes: Mesoeucrocodylia) from the Late Cretaceous of Madagascar. Historical Biology 18:255–369.
- Turner, A. H., and G. A. Buckley. 2008. *Mahajangasuchus insignis* (Crocodyliformes: Mesoeucrocodylia) cranial anatomy and new data on the origin of the eusuchian-style palate. Journal of Vertebrate Paleontology 28:382–408.
- Turner, A. H., and J. O. Calvo. 2005. A new sebecosuchian crocodyliform from the Late Cretaceous of Patagonia. Journal of Vertebrate Paleontology 25:87–98.
- Turner, A. H., and J. J. W. Sertich. 2010. Phylogenetic history of *Simosuchus clarki* (Crocodyliformes: Notosuchia) from the Late Cretaceous of Madagascar. Society of Vertebrate Paleontology Memoir 10:177–236.
- Walker, A. D. 1970. A Revision of the Jurassic Reptile *Hallopus victor* (Marsh), with remarks on the classification of crocodiles. Philosophical Transactions of the Royal Society of London, Series B 257:323–372.

Submitted June 8, 2011; revisions received October 17, 2011; accepted November 28, 2011.

Handling editor: You Hailu.